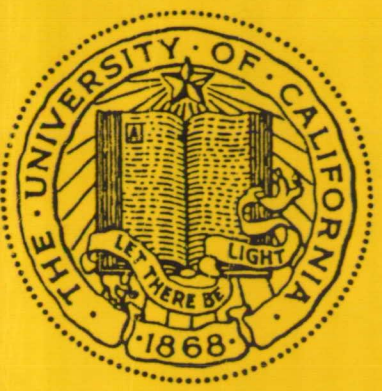

STRUCTURAL SYSTEMS
RESEARCH PROJECT

Report No.
SSRP - 90/03

COMPARISON OF NASTRAN ANALYSIS WITH GROUND VIBRATION RESULTS OF UH–60A NASA/AEFA TEST CONFIGURATION

Final Contractor Report for NASA ARC Contract NCC2-598

by

Florentino Idosor
Frieder Seible

September 1990

Department of Applied Mechanics
and Engineering Sciences
University of California, San Diego
La Jolla, California

STRUCTURAL SYSTEMS
RESEARCH PROJECT

Report No.
SSRP - 90/03

COMPARISON OF NASTRAN ANALYSIS WITH GROUND VIBRATION RESULTS OF UH–60A NASA/AEFA TEST CONFIGURATION

Final Contractor Report for NASA ARC Contract NCC2-598

by

Florentino Idosor
Frieder Seible

September 1990

Department of Applied Mechanics
and Engineering Sciences
University of California, San Diego
La Jolla, California

University of California, San Diego
Structural Systems Research Project

Report No. SSRP-90/3

COMPARISON OF NASTRAN ANALYSIS WITH GROUND VIBRATION RESULTS OF UH–60A NASA/AEFA TEST CONFIGURATION

Final Contractor Report for NASA ARC Contract NCC2-598

by

FLORENTINO IDOSOR
Graduate Research Assistant

and

FRIEDER SEIBLE
Professor of Structural Engineering

September 1990

Department of Applied Mechanics and Engineering Sciences
University of California, San Diego
La Jolla, California 92093

Abstract

Preceding program flight tests, a ground vibration test and modal test analysis of a UH-60A Black Hawk helicopter was conducted by Sikorsky Aircraft to complement the UH-60A test plan and NASA/ARMY Modern Technology Rotor Airloads Program. The 'NASA/AEFA' shake test configuration had been tested for modal frequencies and shapes and compared with its NASTRAN finite element model counterpart to give correlative results. Based upon previous findings, significant differences in modal data existed and were attributed to assumptions regarding the influence of secondary structure contributions in the preliminary NASTRAN modeling. An analysis of an updated finite element model including several secondary structural additions (ie. cockpit doors, transmission bridge, etc.) has confirmed that **the inclusion of specific secondary components produces a significant effect on modal frequency and free-response shapes and improves correlations at lower frequencies with shake test data.**

Table of Contents

List of Tables

List of Figures

ROTORCRAFT DESIGN PHILOSOPHY & APPROACH

The structural analysis of a modern rotorcraft is preceded by an understanding of the iterative design process. The process of design seeks to maximize specific performance/mechanical characteristics of the structure while minimizing others. The methods employed are often dictated by expected loading quantities. The basis for many structural design approaches are defined by the following limit, yield, and ultimate load concepts: **Limit Loads** are the maximum loads anticipated on the vehicle during normal flight operation. The structure shall be capable of supporting limit loads without undergoing excessive elastic or plastic deformations. Loads greater than limit loads can be designed for. Unfortunately, the greater load capacity would introduce an increase in structural weight and cost and a decrease in payload capacity. **Yield Loads** induce stresses that will produce a small amount of permanent deformation. Elastic behavior is exhibited in structural members below the yield strength. Above yield strength, plastic deformation begins. In most cases, the yield load is set equal to limit load. **Ultimate Loads** induce the maximum stress value in the structural material. Just below the ultimate strength, strain hardening of the ductile material is observed. After ultimate strength has been reached, necking may occur in tensile members. Continued plastic behavior after this point will lead to member failure. The structure shall be designed to carry certain ultimate loads without failure. Thus, ultimate loads are equal to limit loads multiplied by an ultimate factor of safety (i.e. FS=1.5). Increased safety factors may also be used depending on the mission or operational requirements. The extra reserve of strength created by the safety factor will also account for variables such as: 1) approximations in aerodynamic and structural theory/analysis 2) variations in the physical properties of materials and 3) differences in construction and inspection standards.

Since yield loads correspond to limit loads in most cases, two forms of design approaches are consistently seen in the aerospace industry: limit load design and ultimate load design. Thus, two design methods are described: one governing elastic theory exclusively, and the other accounting for elastic and plastic behavior. Unlike other structural design/analysis disciplines such as reinforced concrete design where only one form of design is chosen (either a working stress or ultimate strength design), a rotorcraft production may rely on a combination of both methods for overall design. At the minimum, structural members must carry all limit loads

while optimizing **weight, strength,** and/or **fatigue** characteristics. At the maximum, important components, such as engines, transmission support structure, or landing gear, that must endure critical flight or environmental situations, may be designed for ultimate loading. The standards governing the use of limit load or ultimate load design depend greatly on any military specifications (i.e. MIL-S-8698, Structural Design Requirements, Helicopter) or civilian criteria (i.e. FAR 29, Federal Aviation Requirements) which may be imposed on the production rotorcraft. Thus given a specific design approach, a complete stress analysis must accurately estimate the load capacity of its structural members to minimize weight and cost as well as maximize strength and fatigue characteristics in a time efficient manner. Given a large and complex structural system, in terms of physical geometry and the use of diverse metal and composite materials, this estimation becomes a difficult task and requires advanced methods (ie. finite element techniques) other than previous semi-empirical "industrial cookbook" or "hand" methods (ie. shear and moment diagrams). From the formulation of these static models to calculate the load or stress *failure condition* of the rotorcraft, a basic dynamic model must be evolved to predict the vibratory *'in-service' condition.*

BACKGROUND

DAMVIBS PROGRAM

With the U.S. rotorcraft industry's recent capability to accurately calculate static characteristics of helicopter fuselage structures, the even greater dynamic design problem of vibration prediction and control still remains. Significant vibration decreases overall vehicle performance and flight safety, increases maintenance efforts, and is of great concern in terms of human factors. On numerous occasions, inaccurate analytical predictions have led to costly "quick fixes" and unwelcome compromises in design detail.

Several programs have contributed to the development of rotorcraft finite element models and their predictive capabilities. One recent advance in assessing the requirements for definitive vibration prediction and control comes from Phase I of the continuing DAMVIBS program. To achieve a superior capability in utilizing finite element models to support the Country's industrial design of helicopter airframe structures, NASA Langley Research Center sponsored the DAMVIBS program (**D**esign/**A**nalysis **M**ethods for **VIB**ration**S**) with industry and academia in the early 80s to present day. Major technological contributions were received from the four industrial participants: Boeing-Vertol, McDonnell-Douglas Helicopters, Bell Helicopter-Textron, and Sikorsky Aircraft. Each participant discussed, planned, and modeled a large scale finite element model of its chosen rotorcraft. Shake tests and modal test analyses were subsequently performed and compared with the analytical model. A current summation of results from this program indicates that significant deficiencies exist in the development of rotorcraft FE models and their subsequent correlations with experimental results. It has also demonstrated the need for improved basic finite element modeling guidelines, efficient computational and generic analytical procedures, and commonly accepted methodologies in treating this unique structural dynamics problem.

Sikorsky Aircraft's contribution to the DAMVIBS program comes through its development and continuing refinement of the UH-60A Black Hawk finite element model. Sikorsky's NASTRAN model of the UH-60A DAMVIBS baseline weight and primary structural configuration is the analytical foundation and fundamental

starting point for the current improved NASTRAN model which includes secondary structural components and a modified "NASA/AEFA" flight weight distribution as prescribed by the NASA/ARMY Modern Technology Rotor Airloads Program.

MODERN TECHNOLOGY ROTOR AIRLOADS PROGRAM

Currently, NASA and the U.S. ARMY are sponsoring the Modern Technology Rotor Airloads Program (MTRA Program), with industry and academia to experimentally define vibratory airloads for the:

Validation of CFD and Comprehensive Rotorcraft Codes
Investigation of Unique Flow Phenomena
Modernization of Industry Empirical Design Methods

Hence, a comprehensive database will be formed to validate the techniques and methodologies required to improve the performance, dynamics, acoustics, and handling qualities of civil and military rotorcraft. A justification for this research consists of past acoustic, aerodynamic, aeroelastic, and several interdisciplinary studies recognizing rotor system vibratory airloads as the main source of rotorcraft noise and vibration.

The key element of the MTRA Program is the UH-60A Black Hawk test plan (also known as the UH-60A Airloads Program) which will further evolve the database of the modern rotor through numerous flight tests, model scale, and full scale wind tunnel tests for rotor airload definition in conjunction with the development of specific code applications for analytical prediction and correlation (ie. NASTRAN modal prediction/correlation). The following ground vibration test and finite element analysis/comparison serves as a complementary contribution to the UH-60A test plan. The UH-60A NASTRAN model will be periodically revised for the improvement of overall predictive capabilities and for specific applications in support of the MTRA Program and UH-60A test plan. Through the validation and continuing improvement of a predictive analytic model, a generic understanding of inherent fuselage characteristics may be achieved. Ultimately, their role within rotor-fuselage coupling behavior may be characterized and resulting overall vibration may be controlled in design.

GENERAL INTRODUCTION

To support the Modern Technology Rotor Airloads Program and UH-60A test plan, the UH-60A Black Hawk Helicopter has undergone a series of comprehensive experimental and analytical tests to determine accurate dynamic characteristics of the fuselage structure. Preceding program flight tests at the U.S. Army's Aviation Engineering Flight Activity (AEFA, Edwards Air Force Base, California), a ground vibration test (GVT) and subsequent modal test analysis was conducted by Sikorsky Aircraft using an equivalent *flight weight configuration henceforth denoted as "NASA/AEFA"*. The NASA/AEFA GVT article was tested for modal frequencies and shapes and compared with its NASTRAN finite element model counterpart. Previous undamped results showed significant differences in modal response data. These differences could be attributed in part to modeling assumptions made concerning the influence of secondary structural components. Secondary components such as firewall, transmission bridge, cockpit doors, etc. were not part of the analytical model of primary structure.

In this report, an analysis of a second, updated NASTRAN model including various secondary structural components is described and their effect on the modal response characteristics of the UH-60A Black Hawk Helicopter is assessed.

TEST CONFIGURATIONS

DESCRIPTION OF SIKORSKY UH-60A BLACK HAWK HELICOPTER

The UH-60A Black Hawk Helicopter is a single rotor helicopter design for the transportation of troops and cargo with an operational gross flight weight of 22,000 lbs. The aircraft is designed to normally carry 11 and up to 14 fully equipped troops with a high density seating arrangement plus a crew of three: pilot, copilot, and crew chief. The helicopter has a large cabin which enables it to be used without modification for medical evacuation, reconnaissance, command and control purposes, or troop resupply. For external-lift missions, its cargo hook has a capacity of up to 8,000 lbs.

The main rotor system consists of four blades with a fully articulated elastomeric bearing main rotor head. The craft has main and tail rotor diameters of 53 ft., 8 in. and 11 ft. , 0 in., respectively with a fuselage length of 50 ft., 3/4 in. Directional control is provided by a four bladed tractor tail rotor mounted on the top right hand side of the tail rotor pylon. Normal main and tail rotor speeds are 258 rpm and 1190 rpm respectively. The UH-60A has a 373 mile range and cruises at a speed of 145 kts with a maximum level speed of 160 kts. The primary power is supplied by two 1,151 kW General Electric T700-GE-700 advanced-technology turboshafts located above and on each side of the aft portion of the mid cabin.

Fuel is carried in two large crashworthy self-sealing fuel tanks located in the transition section. The landing gear consists of main wheels on each side of the fuselage and a tail wheel. The oleo struts of the three wheels operate as normal air-oil struts in normal landing but are designed to stroke at constant load in crash conditions with high vertical impact velocities. The struts are also used to lower the aircraft until it almost contacts the ground to allow for air transportation in aircraft with limited ceiling height. Just aft of the tail wheel is a splice in the tailcone which allows manual folding of the tail rotor pylon. One helicopter can be accommodated in a C-130 transport aircraft, two in a C-141, and six in a C-5A. The UH-60A horizontal stabilator is moveable with the angle of attack being controlled by a linear electrical actuator mounted within the tail rotor pylon and attached to a fitting on the upper surface of the stabilator.

The UH-60A is intended to serve as the U.S. Army's primary combat assault helicopter. Its mission adaptability has allowed it to perform under different configurations within other branches of the rotorcraft community such as the U.S. Navy, Coast Guard, and Drug Enforcement Agency.

DAMVIBS BASELINE CONFIGURATION

UH-60A ground vibration testing was conducted by Sikorsky Aircraft in Stratford, Connecticut. NASA/AEFA shake testing for the Modern Technology Rotor Airloads Program was performed in conjunction with similar tests for the DAMVIBS Program. After the baseline DAMVIBS UH-60A was tested for various modal response functions and parameters, equivalent masses of flight components were added at specific locations to duplicate the NASA/AEFA flight weight distribution and retested. The NASA/AEFA GVT was finally conducted using this weight and structural configuration. The baseline DAMVIBS GVT article is described as a flight worthy, government owned UH-60A helicopter (S/N 86-24507., No. 640) with the following parts and equipment removed:

Main rotor blades	Tail rotor blades
Main rotor hub	Tail rotor hub
Spindles	Cabin troop seats
Bearings	Tail gearbox cover
Dampers	Intermediate gearbox cover
Bifilar	Nose absorber access cover
Lower pylon fairing	Various aerodynamic fairings/covers
Fuel	

Various aerodynamic fairings and covers were removed to allow access to measurement locations. The presence of most secondary structural components intact in both GVT articles is noted. For both DAMVIBS and NASA/AEFA GVT configurations, the nose, forward cabin, and aft cabin vibration absorbers were rendered inactive. The following are installed in the DAMVIBS GVT article:

Modified Black Hawk main rotor hub

Main rotor head ballast
Main & tail rotor excitation hardware
Main & tail rotor suspension hardware
Dummy tail rotor hub

Six hundred forty pounds were added to the main rotor hub, in the form of main rotor head shaker hardware and dummy steel plates at hub arms, to simulate the removed bifilar mass and 50 percent of the flapping mass of the main rotor blades. Thus, the GVT article rotor head mass will be equal to the static (non-flapping) mass of the aircraft rotor head plus 50% of the dynamic main rotor blade mass (flapping). These additions to the main rotor hub are effected to *approximately* simulate the 4/rev rotor impedance of the UH-60A, and to consequently yield test modes near the 4/rev region with properties similar to the modes of an in-flight aircraft which has frequencies in the 4/rev region.

As was done with the main rotor hardware, the tail rotor hub and blades were replaced by an equivalent hub mass modified to include an attachment for tail suspension and have equivalent lumped mass and inertia properties.

NASA/AEFA GROUND VIBRATION TEST CONFIGURATION

To satisfy the NASA/AEFA flight test weight distribution requirement as defined by the MTRA Program, the *equivalent* masses of the following flight components were added to the DAMVIBS GVT article for modal testing (figure 1):

Pilot
Copilot
Ballast
Full Fuel (actual)
Instrumentation Racks (3)

One notes that these additions to the GVT article effectively change mass distribution only (ie. the stiffness contributions from the addition of true flight test components such as instrument racks, ballast rack, etc. is unreflected in GVT and NASTRAN data). The sole difference between the NASA/AEFA and DAMVIBS GVT configurations is the

addition of the component masses mentioned above. The NASA/AEFA shake test configuration weighs approximately 17,800 lbs. with the addition of the seven components, while the base DAMVIBS shake test article weighs 10,140 lbs.

GROUND VIBRATIONS TESTING

TEST DESCRIPTION & OBJECTIVES

Several objectives and requirements are maintained for the NASA/AEFA ground vibration test. Among the objectives are the gathering of modal data leading to the extraction of free-response quantities such as resonant shapes/frequencies, damping levels, and frequency/time domain response functions. A statement of minimum loading excitation levels and their corresponding frequency ranges used by inertial actuators is required, as is the placement and orientation of these excitations. The accurate gathering of data must be accomplished using existing computational software and hardware and it should be done in a time efficient manner for the on-site review, interpretation, and plotting of data. Another GVT requirement is the selection of specific correlation points and the coincidence of accelerometer measurement locations with NASTRAN model grid points. In addition, a specific form of suspension is needed to simulate the free-free dynamic response condition of the in-flight aircraft.

AIRCRAFT SUSPENSION SYSTEMS

The test article was suspended from overhead support I-beam trusses by a series of spring packs made from elastic bungee cords, chain hoists, and long steel cables at both the main and tail rotor hubs (figure 2). This was done to simulate the 'free-free' analysis condition which simulates the in-flight aircraft free of grounding restraints. The spring packs also act as soft springs to isolate the GVT article from overhead supports and provide for article rigid body modes of less than 1.5 Hz.

GVT results have shown that the bungee system was subject to modes of the "plucked string" variety which had a significant effect on shake test frequency response measurements for the DAMVIBS GVT article. Without the presence of the suspension system, it was expected that only one peak indicating the fuselage 1st lateral bending mode would occur in the 5 to 6 Hz region. However, when the aircraft was excited laterally, two and sometimes three closely-spaced resonance

peaks were observed in the region. The peaks were found at 5.3, 5.5, and 5.7 Hz for the DAMVIBS configuration. The bungee systems (local lateral cables) of both forward and aft suspension systems were being excited and were coupling with the 1st lateral bending mode to produce three coupled fuselage/bungee modes. A brief attempt was made to lower the frequencies of the cable modes by adding weight and by removing bungee strands. Shifting these frequencies proved difficult to do and the effort was abandoned due to lack of time. No evidence of the cable modes was observed at higher frequencies. Tests after the NASA/AEFA and DAMVIBS GVT were conducted with an instrumented bungee system to characterize these anomalous effects. We note that the inclusion of the bungee systems into the finite element models to be discussed has been made to reflect the correction of any comparative anomalies.

Ceiling supports were shown to make little or no contribution to the measured airframe response by acceleration measurements of the overhead trusses. Response of the test facility ceiling near the attachment points of the suspension system were measured during vertical excitations. Minor vertical responses in the forward ceiling support due to main rotor excitations in the 14 to 18 Hz range did not appear to influence any of the structural modes of the DAMVIBS configuration fuselage. Lesser responses were encountered in the aft ceiling support for vertical tail rotor excitations.

APPLIED LOAD EXCITATIONS

Longitudinal, lateral, and vertical forces as well as pitching, rolling, and yawing moment excitations were achieved through the proper alignment of the shakers. Vibratory loads induced by swept, step since force inputs were applied with the use of two electrohydraulic inertia actuators placed at the main rotor hub on opposite arms of the aircraft hub and one actuator placed at the tail rotor hub. Thus, there are two excitation locations at the main and tail rotor heads.and three excitation orientations for the actual test setup (table I). The shakers are high performance servo controlled actuators with closed loop displacement feedback systems which resulted in a shaker force that varied over the frequency range of excitation. Applied shaker forces at the main rotor hub were calculated from the measured acceleration of the shaker moving mass while the input shaker forces at

the tail rotor were measured with a proving ring load cell and reacted by a large reaction mass at rest on the floor.

The force level of excitation is based on the practical considerations of response magnitude, nonlinear response, and the behavior of the shaker through resonances involving large motions at the rotor head. Ideally, the magnitude of the applied dynamic loads should be as large as possible, up to the levels of operational loads. A sinusoidally driven external weight force level of 100 lbs. was used for most of the test although other force levels ranging from 50 to 200 lbs. to as high as 550 lbs. were applied to investigate nonlinear response.

The selection of the frequency range of main rotor head excitation is motivated by the UH-60A's 4/rev blade passage frequency of 17.2 Hz. It ranges from 0.2 to 2.2 times the 4/rev frequency with the approximate range from 3.4 to 37.8 Hz or for practical considerations, 0 to 45 Hz to identify rigid body modes and clear the highest contributing frequency to modal response for the NASA/AEFA configuration. A similar frequency range selection is chosen to cover the 4/rev forcing frequency range of the tail rotor blades from 3 to 80 Hz.

The use of the second excitation location at the tail rotor hub was proposed for the measurement of response modes not adequately defined from main rotor head excitations. The servo-controlled hydraulic actuator at the tail rotor hub actuator was attached to an aluminum fitting at the centerline of the stabilator attachment lugs. Unfortunately, its use was limited to preliminary checks and secondary investigations due to test scheduling restrictions. Two vertical excitation sweeps were performed to provide a preliminary evaluation of measurement systems and various test techniques prior to real time data acquisition and to characterize the airframe response. Valid reciprocity checks were conducted with the main rotor excitations as well as the measurement of additional elements of the frequency response function matrix to serve as an additional check of modal parameters and to assess the extent of nonlinearities in the aircraft response. Lateral excitations were also performed in the same fashion with the shaker attachment location at the tail tie down fitting located at the base of the tail pylon.

DATA ACQUISITION & ANALYSIS SYSTEMS

The gathering of modal test data requires the use of existing test transducers, computational hardware, and software. Seventy-two locations were selected as measurement locations to coincide with NASTRAN finite element model grid points to fully define fundamental mode shapes of the airframe and major components. Correlations and modal surveys were made using 32 of these points by Sikorsky Aircraft for the NASA/AEFA GVT. The measurement locations were dispersed throughout the test structure with an emphasis in the forward and aft cabin sections at major frames, stringer, and beam intersections (figure 3). Accelerometer mounting blocks were bonded at these locations, allowing the timely installation and removal of accelerometers which attached to the blocks with threaded studs. The corresponding NASTRAN grid points were modified, if necessary, to reflect the true measurement locations for correlation. For both DAMVIBS and NASA/AEFA ground vibration tests, the following dynamic test and analysis systems were utilized (figure 4):

Solartron 1250 18 Channel Frequency Response Analyzer
consists of: 2-Channel Frequency Response Analyzer
8-Channel Frequency Response Analyzer Extensions (2)

Solartron 2 Channel FFT Spectrum Analyzer

Hewlett Packard 9836 Computer and Peripherals
consists of: Winchester 14.5 Mb Disk
Hewlett Packard-7475A 6-Pen Plotter
Hewlett Packard-2673A Graphics Printer

Imperial College of Science & Technology System Control/Analysis Software

SMS Modal 3 SE Control/ Analysis Software

Quantities such as modal deformation shapes, resonant frequencies, and frequency domain data were computationally extracted with the use of two different system control and analysis programs from the Imperial College of Science and Technology and SMS.

ANALYTICAL MODELS

REVIEW OF NASTRAN PRIMARY/SECONDARY STRUCTURAL SYSTEMS

Preceding the final comparison with NASA/AEFA modal data, two NASTRAN finite element models describing the shake test configuration were developed and studied for changes in modal frequency and shape. The first FEM describes **primary structure** of the fuselage exclusively. Generically defined, primary structures are components that are designed to be load carrying members. Primary structure consists of aluminum semi-monocoque structure including frames, stringers, skins or panels, beams, and bulkheads. In areas of high temperature or concentrated load, titanium and machined parts are used, respectively. Generally, the airframe is built up from extruded stock. The finite element model for this primary structural system is composed of 8,819 elements, specified geometrically by 4,669 grid points, and utilizes 25,509 degrees of freedom (DOF)(figure 5). By various modal reduction methods, the number of global DOF's are decreased to approximately 60 modal coordinates depending on the frequency range of eigenvalue extraction.

The second, revised FEM combines both the **primary structure and specific secondary structural components.** Generally, glass, plexiglass, fiberglass, and kevlar coverings or skins fall into the secondary structure category. They are generally formed in a composite sandwich construction made up of aluminum honeycomb cores with laminated fiberglass or kevlar skins. In some areas, the aluminum core is not used with the fiberglass and kevlar skins. The windows in the midcabin and cockpit, except for the windshields in front of the pilot and copilot are stretch plexiglass. The windshields, which have wipers, are laminated glass inside with an outside layer of PVB plastic. Examples of secondary components are given in figure 6 The primary and secondary structural system is discretized by 9,742 elements, geometrically described by 4,379 grid points, and requires 26,547 DOF's (figure 7). By similar reduction methods, the number of DOF's are decreased to a smaller modal subset. Both NASTRAN models have an equivalent weight of 17,800 lbs (including lumped masses of pilot, copilot, fuel, ballast, and instrumentation racks). The models are analyzed with the use of the MSC NASTRAN structural analysis package and Cray Y-MP/832 supercomputer located at NASA-Ames Research Center.

In addition to the selected secondary structural components, several modeling revisions are included to correct physical and material properties of the former primary structure FEM. For this modified FEM, the following revisions/additions were made:

Added Firewall
Added Transmission Bridge
Revised Shell Properties for Transmission
Simulated Windshield
Gunner's Window Approximation
Simulated Cockpit Doors
Cabin Doors Approximation
Revised Stabilator Springs

Although all secondary structural components may be modeled, a few key components are projected to contribute much greater stiffness effects to the static and dynamic models in comparison to other components. In modeling revisions then, priority must be given to those components that are thought to cause significant changes in fundamental dynamic response modes. The above mentioned modifications are motivated by two studies conducted in the post-DAMVIBS testing phases.

DEVELOPMENT OF SECONDARY COMPONENT STUDY

The first inquiry pertaining to secondary components and analytical structural stiffness effects came directly after DAMVIBS shake testing. A review of analytical mode shapes and test results indicated that the DAMVIBS baseline NASTRAN model appeared to be weak in the midcabin area and transmission support structure as demonstrated by a lack of correlation of the transmission pitch and second vertical bending modes. A sensitivity analysis was conducted to *approximate* the effects of a full finite element discretization of the cabin doors for the model. Several simple analysis cases were conducted using "steel cable" approximations of various dimensions connected to the opposite corners of the door openings. Cross sectional areas were varied from 0.000196 to 1.77 in^2. Changes in mode shape frequency

placement for the configuration became evident as the cross sections were increased (figure fem model modifications sensitivity analysis). The cabin door simulation proved to be favorable in decreasing the frequency percent errors of the second and third vertical bending modes as seen in table II. Thus, a chief assumption of the study is supported by previous DAMVIBS work suggesting that minor changes in stiffness resulting from additional secondary components in the analytic model will give improved correlations with GVT data.

The second study was conducted by Sikorsky Aircraft in recent support of UH-60A and EH-60A aircraft production efforts for the Army and related design programs. Most of the secondary components and modeling revisions are motivated by the Sikorsky study using a non-linear optimization programming code called PAREDYM (PArameter REfinement of DYnamic Models), which identifies the structural changes required in a finite element model to yield improved correlations with GVT results. The following relation describes the basic formulation of the optimization program:

$$\{ \Delta Y \} = [T] \{ \Delta B \} + \{ R \}$$

where

$\{ \Delta Y \} = \{ Y_e \} - \{ Y_a \}$	Difference between analytical and experimental data Generally containing eigenvectors and eigenvalues
$[T]$	Sensitivity matrix with respect to design parameters
$\{ \Delta B \} = \{ B_r \} - \{ B_o \}$	Difference between revised and original design parameters
$\{ R \}$	Residual vector summing errors arising from: Truncation of Taylor series (non-linear effects) Incomplete design parameter selection Experimental errors

The sensitivity matrix is defined specifically by:

$$[T] = \begin{bmatrix} \delta Y_1/\delta B_1 & \delta Y_1/\delta B_2 & . & . & \delta Y_1/\delta B_m \\ \delta Y_2/\delta B_1 & . & . & . & . \\ . & . & . & . & . \\ . & . & . & . & . \\ \delta Y_n/\delta B_1 & . & . & . & \delta Y_n/\delta B_m \end{bmatrix}$$

where n = number of modal data points
m = number of design parameters

The formulation relates differences in modal shapes and frequencies to finite element model parameters using a first order Taylor series expansion thus defining a system of equations involving first order derivatives or sensitivities. The PAREDYM program utilizes NASTRAN solution sequences and DMAP formats for normal modes and design sensitivity analysis under FORTRAN control for iterations and input/output routines. Basically, PAREDYM first extracts eigensolutions of the NASTRAN model, $\{Y_a\}$, and computes eigensolution sensitivities, [T], with respect to design parameters, {B}. The selected design parameters refer to finite element properties such as element thicknesses, cross sectional areas, etc. that are subject to modification. The code also converts shake test data to an equivalent NASTRAN format, $\{Y_e\}$, such that a similar comparison database is created for subsequent matrix computations. Given mode shape/frequency differences between analysis and test, the sensitivity matrix, and original design parameters subject to systematic modification, the code will compute the element modifications, $\{\Delta B\}$ (and thus $\{B_r\}$) and estimate the residual errors, {R} (depending upon matrix characteristics and solution method), needed to minimize the modal differences, $\{\Delta Y\}$. Using the revised model, PAREDYM will then recalculate the eigensolution, new mode shape/frequency differences, and sensitivity matrix. While continually updating the model and recalculating the analytical and sensitivity quantities, the solution process will iterate towards the minimization of test/analysis differences until convergence criteria are met. The method of solution will depend upon the number of design parameters, number of modal data points, and other properties of the matrix formulation. Specific model optimizations suggested by the PAREDYM code *are not*

incorporated into the final UH-60A improved model however. The structural modification suggestions *are used instead as guidelines* in making justifiable structural additions and modeling revisions (ie. secondary structure, stabilator improvement) based upon physical modeling principles. The PAREDYM code is currently limited to locating the areas deficient in terms of stiffness and defining the qualitative model changes that must be effected if they can be physically warranted. Sikorsky Aircraft plans to build upon the theoretical, computational , and practical aspects of the refinement code. The PAREDYM code, developed by I.U. Ojalvo and T. Ting of the University of Bridgeport, is based on J.D. Collins' original method regarding the statistical identification of structures

MODEL OVERVIEW

Structural Model

The connectivity, material properties, and dimensional characteristics of structural members of the UH-60A Helicopter are discretized analytically through the formulation and selective combination of several basic finite elements. A general overview of those elements used to represent the general substructures of the UH-60A such as frames, aerodynamic shells, pylons, etc. is presented.

Quadrilateral plate elements or CQUAD4s represent a significant percentage of the total number of elements that compose the UH-60A structural models. These shell elements are characterized by the coupling of bending and membrane stiffnesses and thus may be subject to bending and twisting moments in addition to shear and normal forces. For the representation of UH-60A primary and primary/secondary structural systems, **8,803** to **9,742** finite elements are required respectively. The CQUAD4s number **3,240 / 3,309** (Primary / Primary & Secondary) and are used consistently to model the repeated fuselage frames, bulkheads, and skins including the following structures (figure 8):

External stores support structure (ESSS)
Transmission and engines
Firewalls

Tailcone skins
Tail rotor pylon structure
Stabilator fairings

For the specific case of UH-60A structural dynamics, skins of the vibration model are treated as a material which has both in-plane shear and in-plane stiffness to maintain the assumption of unbuckled (fully effective) skin in mild flight maneuvers. In a previous static model leading to the development of the dynamic model, skins were once treated as shear only material in keeping with the assumption of buckled skin in severe maneuvers. Thus, a difference in skin effectiveness is found between the current vibration model and its predecessor static model.

Triangular plate elements or CTRIA3s are used in place of CQUAD4s to describe highly curved, warped, or swept surfaces. CTRIA3s are commonly used to represent nonrectangular sections in modeling difficult or complex geometries. These shell elements, also characterized by the coupling of bending and membrane stiffnesses, may undergo bending and twisting moments in addition to shear and normal loads behavior. CTRIA3 elements, which total **836 / 878** (Primary / Primary & Secondary) in number, supplement the CQUAD4 quadrilateral plate discretization of frames, bulkheads, and skins in the UH-60A models (figure 9).

Uniaxial bar elements or CBARs may exhibit extension, torsion, and bending behaviors and may thus be subjected to torque and bending moments in addition to shear and axial forces. For the UH-60A models, **4,718 / 5,510** (Primary / Primary & Secondary) uniform bar elements are used repeatedly in the discretization of buttline beams, beam flanges, and web stiffeners for the UH-60A's frames and bulkheads (figure 10). CBARs are also found in the discretization of the following:

Main rotor shaft
Tail rotor pylon structure
Stabilator
Main and tail landing gear
Cockpit door/window supports
External Stores Support Structure (ESSS)
Firewall

Cockpit windshield/door approximation

They are commonly used in the modeling of longerons and stringers which are subject to axial and transverse bending loads.

Rods or CONROD elements ,which are subject to axial extensions and torsional behavior exclusively, are unique extensions of the simple beam element. Because these structural elements are easily modified in terms of variable stiffnesses and cross sectional areas within the NASTRAN data decks, they are used in a limited capacity for the approximation of cabin door, gunner windows, main and tail rotor bungee suspension systems. There are **6 / 41** (Primary / Primary & Secondary) such members .

Elastic springs or ELAS2 elements scalar spring elements are useful for representing elastic properties that cannot be conveniently modeled with the usual metric structural elements (elements whose stiffnesses are derived from geometric properties). The stiffness coefficient of the scalar element may be directly specified without reference to dimensional and material properties (ie. area moment of inertia, element length, Young's modulus, etc.). Allowance for the specification of spring stiffnesses between degrees of freedom is helpful in the approximation of spring-type mechanisms where dynamic behavior is unclear and an analytical estimation is required. For both the primary and primary/secondary structural systems, **4** ELAS2 elements are used in the discretization of stabilator isolation springs.

Mass Model

The analyst is presented with the tedious and time consuming task of distributing structural and nonstructural weight to the appropriate areas of the finite element model. In the case of rotorcraft, most weight is of a nonstructural nature. Automated procedures with a NASTRAN interface program are used in industry to generate the necessary NASTRAN input data.

The mass model is generated by first creating a computer file listing the weight and inertia properties of approximately 5,000 components (both structural and nonstructural) in a MIL-STD tabulation form. Hence, a description of the item

(ie. pilot, cabin seat, frame section, etc.), its mass, centroid location, and mass moments of inertia, in terms of the model coordinate system are stored. Second, a volume describing the entire aircraft, again using the model coordinate system, is defined in the mass model generation program and divided into a greater number of smaller, equally sized subvolumes or regions. The interface program assigns each mass item a location in the model volume and respective region based on its centroidal coordinates. Next, the program calculates a new center of gravity and single lumped mass from the summation and computation of mass items data for each region. Finally, NASTRAN input data lines are written specifying a grid point (GRID) and concentrated mass (CONM2) at the new centroid of each region. This process is repeated for each region over the entire volume. Another RBE3 rigid element is specified "by hand" for each concentrated or lumped mass to connect the concentrated mass item to the structural model. The RBE3 element allows the mass to undergo components of motion calculated from the average summation or weighted average of other nearby structural grid points. This mass modeling procedure is depicted in figure 11. The volume and region shape may be arbitrarily chosen based upon the unique structural and mass configuration of different aircraft. For example, the UH-60A NASTRAN model by Sikorsky uses a finite pie shaped inertia region, while Boeing-Vertol uses a rectangular box shape for their finite element models. Special mass items may also be input separately "by hand" to represent unique flight components or different weight configurations (ie. NASA/AEFA flight weight distribution).

Damping Model

The analyst is presented with the problem of developing an analytical damping model for the global finite element model based upon the realistic dynamic behavior of the rotorcraft fuselage. For the UH-60A NASTRAN model and others borne of the DAMVIBS program, no damping model is assumed for general modal analyses. A generic understanding of rotorcraft fuselage damping theory and its application to analytical models is currently lacking.

A few practical techniques are used in industry to make a crude estimation of modal damping levels. One standard practice is to assume a 'straight line' critical damping ratio ranging from 2.0 to 2.5% across the frequency range of interest The

initial ratio estimate is based on the analyst's experience with the particular design type and configuration., flight tests results, or vibration experiments. The estimate is then incorporated into eigenvalue extraction procedures to calculate the mode shapes and frequencies of the fuselage model. Another current practice involves the incorporation of critical damping percentages or ratios for each mode in the finite element model after several approximations from various vibration excitations and actuator orientations of the modal test can be averaged. However, such linear or tabular assumptions cannot be utilized in the pre-prototype design process since such damping data is needed 'a priori' to prototype building and shake testing. While the inclusion of "mode to mode" damping ratios from shake tests may be seen as an acceptable method for model validation and has proven to be successful in several correlative studies, such an approach also assumes that the analytical model can find all test mode shapes and frequencies within a specified frequency range with some reasonable degree of accuracy. The approach also assumes that the integrity of the eigensolution extraction is preserved (ie. critical damping ratio approximations do not affect eigensolution of other modes found exclusively in analytical model). Clearly, a damping function and model which is dependent upon structural discretization, connectivity, static, dynamic, and mass characteristics needs to be developed and more importantly understood. A fundamental and generic understanding of physical damping sources and their analytical representation is required for the further development of predictive finite element techniques.

It is noted that the NASTRAN program does not include advanced damping models. For rotorcraft studies, damping in NASTRAN is incorporated through tabular functions of critical damping percentages vs. frequency and the limited use of viscous and structural damping elements.

MODELING CHECK

To attain a certain level of confidence in the finite element discretization, several modeling checks may be performed by the analyst to ensure that the model characterizes the true dynamic behavior of the physical structure. Modeling checks also have the purpose of ensuring the proper representation internal and external constraint conditions in both static and dynamic analyses. Numerous checks have been developed for general rotorcraft finite element analyses through pre-DAMVIBS efforts in industry. Of the several methods available, the *rigid body/enforced displacement check* is the most informative and simplest to apply for the UH-60A dynamic model and warrants a brief description.

The principal purpose of the **Rigid body / Enforced Displacement Check** is to ensure that there are no inconsistent constraints, primarily single point constraints (SPCs), applied to the model. If the dynamic model is placed in a free body condition with no inconsistent constraints present, then it must be capable of undergoing rigid body motions without inducing internal forces.

The NASTRAN model is rigidly constrained at grid points corresponding to the main and tail rotor shaft heads in all translational and rotational degrees of freedom excluding the longitudinal degree of freedom (DOF). Single Point Constraints (SPCs) are used to specify the rigid constraints. In the free longitudinal DOF, a unit displacement is applied to the main rotor shaft (figure 12). This applied unit displacement will yield clearly defined zero displacements and significant force reactions at overconstrained grid points. For correctly unconstrained grid points, including the node specifying the tail rotor shaft head, unit displacements in the longitudinal direction will be computed. Results are easily evaluated from the examination of printed displacement and single point constraint force output. If all grid point displacements on the model are equal to the applied displacements and.all internal forces, including SPC forces, are zero or deemed negligible, then the fuselage model will be unrestricted in translation and rotation motions (table III). Deviation from these conditions will indicate the presence of unspecified constraints. The rigid body/enforced displacement check is also conducted along the other five directional axes.

STATIC STUDY

OBJECTIVES

The main objective of the limited static study is to perform a **preliminary quantification of the effects of added secondary structure** using the two NASTRAN models. Two structural configurations of the NASTRAN UH-60A model are investigated:

1) Primary Structural System

2) Primary and Secondary Structural Systems

Static characteristics (such as displacements and stress concentration redistributions) of these configurations are defined and changes in structural behavior, resulting from the addition of the secondary components and modeling revisions to the primary structure model, become evident. Equivalent static loads, in the form of self weight or uniform gravity loading applied to all concentrated masses in the fuselage, are employed individually in the longitudinal, lateral, and vertical directions to both configurations giving respective deformation and stress states.

CONSTRAINTS

Numerous external and/or internal constraints are required in both static and dynamic analyses. The static load analysis is performed by first imposing external constraint conditions upon the UH-60A fuselage such that rigid body movement is suppressed and several of the problems associated with singular matrices are avoided. In the finite element model, the main rotor shaft head is rigidly constrained in all directions. Thus, the three translational degrees of freedom (DOF) and three rotational DOF will be removed at the main rotor hub. External constraints such as Single Point Constraints or SPCs are defined to specify boundary conditions at the appropriate degrees of freedom by applying a fixed value to a translational or rotational component at a geometric grid point, thus eliminating a percentage of the unwanted degrees of freedom with zero stiffness. Conditions such as the

enforcement of zero motion at a grid point are deemed necessary in a static analysis (ie. constrained main rotor shaft) for the allowance of self weight deflections.

Internal constraints such as Multiple Point Constraints or MPCs are defined to describe linear relationships among displacements between two or more selected degrees of freedom. They are used in the model to approximate the beam or frame connectivity relationships. MPCs are maintained at several grid points between structural elements such as beams and frames (element CBARs and CQUAD4s, respectively) to preserve the design relations and conditions.

Another NASTRAN form of internal constraint used consistently throughout the static and dynamic analyses is the AUTOSPC function. This feature examines the stiffness matrix, locates potentially singular degrees of freedom at the grid point level, and AUTOmatically generates an internal Single Point Constraint at all singular degrees of freedom. This acceptable method of dealing with ill-conditioned matrices for the eventual decomposition, execution, and solution of the matrix formulations *must* be used with single point constraint force output to confirm that reaction forces at the constrained degrees are negligible. Other analytical techniques to deal with the singular stiffness matrix computation such as eigenvalue shifts or grounding restraints using springs with negligible stiffness may be implemented but these methods prove to be time consuming or tedious for large degree of freedom systems.

LOADING

Load magnitudes are taken from NASA/AEFA flight test data stored on the Rotorcraft Technology Branch TRENDS databases. Given a specific flight maneuver (e.g. in hover, level flight, angled maneuvers, etc.), the helicopter centroid will undergo a maximum acceleration and respective increased gravity field or 'self weight' loading in the longitudinal, lateral, and vertical directions. Centroidal acceleration values measured experimentally may be used in computing an equivalent static load quantity, given the UH-60A flight test article mass. Hence, equivalent forces Fx, Fy, Fz may be calculated given the helicopter centroid accelerations AxCG, AyCG, AzCG and the mass of the flight rotorcraft from flight data. These equivalent static loads may be applied to the lumped masses of both NASTRAN

structural configurations in the form of uniform gravity fields specified in one or more of the model axes. Differences in stress and deformation responses between both configurations resulting from the application of equal forces are studied from contour plots of stress concentration redistribution and displacement data. One notes that TRENDS NASA/AEFA flight data acts as a guideline only in defining load magnitudes and their orientations for purposes of static response examination. ..

COMPUTATION METHODS & SOLUTIONS

The static analyses for both finite element models are based on the displacement method. A Gaussian elimination algorithm is employed to find the deformed state solution, given the formulation of the element stiffness matrix and definition of a load vector (in this case, uniform gravity loading). The NASTRAN rigid format Solution 24 for Static Analysis is used.

INFLUENCE OF SECONDARY STRUCTURAL COMPONENTS

The static analyses have shown changes in stress concentrations, strain energies, and structural deformations (figure 13) resulting from the addition of secondary structure. As an ulterior goal, this preliminary analysis will eventually aid in an evaluation of the stiffness of the overall airframe and selected parts of the structural systems (e.g. stabilator, cabin door, etc.) after the development of graphics visualization tools. Information regarding regional stiffnesses will assist in explaining/describing important modes involving torsion, vertical displacements, lateral reponses, or other combinations which will arise in the later real data analysis of the comparison. Both configurations of the NASTRAN model including and excluding secondary structure are studied in describing the static effects of secondary structural additions.

DYNAMIC STUDY

OBJECTIVES

The main objective of the dynamic study is **to quantify the dynamic effects of added secondary structure through the comparison of modal shapes and frequencies from both analytical models.** As in the static study, the two structural configurations of the NASTRAN UH-60A model are investigated:

1) Primary Structural System

2) Primary and Secondary Structural Systems

Dynamic characteristics of these configurations are defined and changes in structural behavior, resulting from the addition of the secondary components and modeling revisions to the primary structure model, become evident. Eigenvector/eigenvalue extractions are performed for each configuration giving respective modal deformation states and resonant frequencies.

CONSTRAINTS

For dynamic analyses, the NASTRAN model is subjected to an unconstrained 'free-free' response condition that simulates the in-flight UH-60A aircraft free of grounding restraints. Hence, external single point constraints are not specified to restrain the structure, thus allowing the eigensolution extraction of rigid body modes of translation and rotation for the free body. The imposition of this condition poses several computational problems such as the decomposition of a singular stiffness matrix. The use of MPC displacement relationships and the AutoSPC function in the generation of internal constraints is continued as in the previous static analyses.

BASIC FORMULATION

An eigensolution extraction does not require a definition of dynamic forces since the formulation of the free response of a single or multi-degree of freedom system is founded upon the following basic relation:

$$[M]\{x\} + [C]\{x\} + [K+iG]\{x\} = 0$$

where
- M = mass matrix
- C = viscous damping matrix
- K = stiffness matrix
- G = structural damping matrix
- x,x,x = respective nodal acceleration,velocity, & displacement vectors

For the undamped case (ie. C = 0, G=0), the solution of the eigenvalue/vector problem leads to a determinantal extraction of the following basic form which may be rewritten in several forms depending upon the extraction method chosen:

$$[K - \lambda M]\{u\} = 0$$

where
- λ = set of eigenvalues (resonant frequencies)
- {u} = set of eigenvectors (mode shapes)

It becomes evident from the formulation of the eigensolution problem for the undamped case, that there exists no dependence on a loading quantity and that the determination of the modal deformation vectors and resonant frequency values are dependent only upon the stiffness and mass matrices and approximations inherent of the chosen reduction and extraction methods.

COMPUTATION METHODS & SOLUTIONS

In the dynamic analyses, emphasis is placed on the use of eigenvalue analysis in yielding the most informative data in the quantification of additional components and the correlation with shake test results. The studies of both NASTRAN models rely on several matrix decomposition, reduction, and computation techniques to compute the eigenvectors (mode shapes) and eigenvalues (resonant frequencies). NASTRAN Rigid Format 3 for Normal Modes Analysis is used with a modified algorithm based on Givens method of tridiagonalization for the real eigenvalue/eigenvector extraction in the free undamped vibrations case. This method is chosen from among the other

basic Givens and Inverse methods for its computational efficiency and accuracy for large, complex degree of freedom systems where numerous eigensolutions are required after extensive static or dynamic matrix reductions are performed.

With greater than 25,500 degrees of freedom specified for each NASTRAN model and restrictions on memory and CPU time, it becomes reasonable to reduce the number of degrees of freedom to a smaller subset, prior to the eigenvalue extraction, which preserves the physical discretization of the actual structure and mathematical integrity of the dynamic formulation. The general method for this type of modal reduction in NASTRAN is called Generalized Dynamic Reduction (GDR) by which a smaller number of modal degrees of freedom are defined on the basis of their modal participation. Generalized Dynamic Reduction is an extension of the static condensation method (Guyan reduction). The number of degrees of freedom in the subset is approximately equal to the 1.5 times the number of roots found below the maximum frequency of interest in the extraction range. In the case of the UH-60A model (0 to 35 Hz, frequency range of interest), approximately 60 degrees of freedom are used. The details of these reduction and extraction procedures is discussed in the referenced NASTRAN manuals.

INFLUENCE OF SECONDARY STRUCTURAL COMPONENTS

Table IV shows changes in NASTRAN mode frequencies with the cumulative removal of secondary components. Generally, slight changes are achieved with the removal such that no one single component can be said to cause a systematic change in all mode estimates with the exception of the cabin door approximation which still warrants a correct discretization based on physical modeling principles before being accepted as part of the 'best estimate' NASA/AEFA NASTRAN finite element model. The effect of secondary components is briefly described:

Simulated Windshield

The approximation of upper and outboard cockpit windshields with beam elements to simulate the local stiffness associated with laminated glass and plexiglass fairings. This approximation which creates additional structural connections

between the cockpit roof and floor in the analytical model have an effect in changing the mode frequency placement of the Transmission Pitch/2nd Vertical Bending , Transmission Roll/Stabilator Yaw, and Transmission Roll/Stabilator Roll modes.

Simulated Cockpit Doors

In place of a full discretization of both cockpit doors, beam elements are utilized in approximating the local stiffness associated with structural aluminum core, kevlar/composite covers, and plexiglass. These double hinged, single piece components are found to affect the the Transmission Pitch/2nd Vertical Bending and 2nd Vertical Bending modes.

Added Firewall

The firewall is fully discretized in the primary/secondary structural model. This main rotor pylon fairing component which lies between the exhaust outlets of the twin turboshafts is an internal component subjected to high temperatures. It is fabricated from built-up titanium sheet stock with a combination of spot welding and riveting. This component effects greatly increases the frequencies of the 1st Vertical Bending, Stabilator Roll, and Transmission Pitch, Transmission Roll/Stabilator Yaw, Stabilator Roll/Transmission Roll, and 2nd Vertical Bending/Transmission Vertical modes.

Added Transmission Bridge

A discretization of the transmission bridge is included in the primary/secondary model. The transmission bridge is a minor set of titanium beams components designed to support the rotor transmission and laterally connect the two firewalls on both sides of the engine. The addition of component is found to affect the Transmission Roll/Stabilator Yaw, Stabilator Roll/Transmission Roll, and 2nd Vertical Bending/Transmission Vertical modes.

Revised Shell Properties for Transmission

In the previous DAMVIBS and EH-60A studies using the primary structure model, several locally-controlled engine forward and aft modes were found. The PAREDYM optimization code suggested doubling the thickness of all plate elements in the main transmission housing to investigate these modes. For these studies, it had a favorable effect on mode correlation although such a change was not based on physical modeling principles. This modeling revision is found to affect the Transmission Pitch/2nd Vertical Bending, Transmission Roll/Stabilator Roll, and 2nd Vertical Bending modes of the NASA/AEFA configuration.

Revised Stabilator Springs

A mode frequency comparison for the increase in stabilator spring stiffness is not offered with this part of the study. The change is considered to be a revision towards the continued refinement and improved modeling of an inherently non-linear component as found in past ground vibration tests.

Gunners Window Approximation

The approximation of small, sliding doors on both sides of the forward cabin are included in the primary/secondary structural model. These laminated glass, composite, and structural aluminum components are represented with respect to stiffness with axial beam elements. This component affects the Transmission Pitch and 2nd Vertical Bending/Transmission Vertical Bending modes. A full discretization of this component may be warranted since it is shown to increase percent errors between analytical and test results.

Cabin Doors Approximation

The approximation of large, sliding doors on both sides of the midcabin are included in the updated model. These components composed of laminated

glass/plexiglass, composite/aluminum sandwich structure, and aluminum sheet are represented by axial beam elements to incorporate lateral and vertical panel stiffnesses associated with door sliders and roller supports. A full discretization of this component may be warranted in the future since it affects the 1st Vertical Bending, Transmission Pitch, Transmission Pitch/2nd Vertical Bending, Stabilator Roll/Transmission Roll, Transmission Roll/Stabilator Roll modes. The inclusion of this approximation causes a significant frequency deviation in the 2nd Vertical Bending/Transmission Vertical Bending mode.

MODAL COMPARISON OF ANALYTICAL MODELS

OVERVIEW OF MODES OF PRIMARY/SECONDARY STRUCTURAL SYSTEM

The primary and secondary structural system represents the most recent and significantly refined finite element model of the UH-60A Black Hawk. Table V describes 38 dynamic response modes obtained from the primary and secondary structural systems in the 0 to 35 Hz range. The first six mode shapes close to 0 Hz are identified as rigid body modes and act as a modeling check corresponding to translational and rotational attitudes. The analysis of undamped modal frequencies and shapes has shown good comparison with test results for modes in the 4 to 17 Hz range. After 17 Hz however, analytical shapes begin to diverge from shake test results. Fundamental modes including lateral or vertical bending components show excellent agreement and improve with the addition of secondary structural components as will be seen. An overview of the significant mode shapes found also in ground vibration tests is presented:

1st Lateral Bending

Figure 14 shows the first analytical mode found after the six rigid body modes. The *1st Lateral Bending* mode is placed at 4.965894 Hz in the P/S structural system. A small 0.43 % increase to this frequency from previous primary structural system estimates is achieved through the addition of secondary components and modeling revisions. Notable lateral deflections about the midcabin section is evident with torsion and roll deflections of the tail rotor pylon. Significant torsion in tail rotor pylon begin after the pylon fold joint. This mode exhibits the first of many anti-symmetric bending behaviors of the stabilator. Stabilator behavior for this mode is accompanied with torsion and yaw rotations. For the frequency range of interest and test accuracy of 0 to 35 Hz, two modes are found to qualify as lateral bending modes for the primary and secondary structural systems.

1st Vertical Bending

The *1st Vertical Bending* mode is placed at 6.047724 Hz in the P/S structural configuration (figure 15). This fundamental shape is signified by major upward vertical deformations centered about the midcabin section. Full fuselage bending as in the previous mode is present. Vertical displacements in the stabilator region are due to the upward deflection of the tail rotor pylon base at fold joint. The P/S structural system shows a 3.87 % improvement in frequency correlation from the primary system estimate of 4.944847 Hz. Under 35 Hz, fives modes qualify as vertical bending modes for the primary and secondary structural systems.

Stabilator Roll

The *Stabilator Roll* mode at 9.956318 Hz is characterized by isolated anti-symmetric bending of the stabilator wing (figure 16). Minor lateral bending in the aft tailcone before the pylon fold joint is present. A minor .91 % frequency increase 9.866302 Hz is brought about through the addition of secondary components. The Stabilator Roll mode is one of seven modes under 35 Hz that include well pronounced and isolated stabilator bending.

Transmission Pitch

This mode shape at 11.25406 Hz is characterized by the pitch rotation of the transmission section and main rotor hub shaft (figure 17). Significant vertical bending in tailcone with anti-symmetric bending of stabilator is present. Longitudinal displacements are found in the tail rotor pylon with additional but limited vertical bending in the cabin areas. A 7.517 % improvement from the previous primary structural system estimate of 10.53568 Hz is achieved through the secondary component additions. Twelve modes in the frequency range of interest some type of pitch, roll, or yaw rotation behavior of the transmission and main rotor hub structures.

Transmission Pitch/2nd Vertical Bending

At 13.07353 Hz, this mode is characterized by notable vertical displacements in the nose and cockpit/cabin transition section to the aft cabin transition section (figure 18). Well defined vertical bending of the fuselage is exhibited as is found in the 1st Vertical Bending mode. Pitching of the transmission shaft is a dominant feature of this mode shape. Full vertical bending of general tailcone section is present. Anti-symmetric vertical bending and yaw rotation of stabilator is also present. From the previous baseline estimate of 11.32761 Hz, a 15.413 % improvement is found.

Transmission Roll/Stabilator Yaw

Although the *Transmission Roll/Stabilator Yaw* mode is characterized by isolated anti-symmetric bending with yaw rotation of the stabilator wing and the limited roll rotation of the transmission structure (figure 19). Isolated and limited vertical and lateral displacements near the cockpit nose and tailcone aft regions are included in this mode. A minor .5257 % frequency increase to 13.75396 Hz from 13.68203 Hz is brought about through the addition of secondary components.

Stabilator Roll/Transmission Roll

The *Stabilator Roll/Transmission Roll* mode at 14.14592 Hz exhibits vertical displacements in the cockpit and tailcone regions (figure 20). Significant displacements are due to rolling of the main rotor hub and transmission support structure. An Anti-symmetric roll and yaw rotation of the stabilator is a prevalent feature of this mode. Minor vertical bending displacements are contributed to the midcabin floor from the rolling of the transmission structure. A 8.539% improvement from previous primary structure model analyses at 13.033 Hz is gained towards the correlation with shake test results.

Transmission Roll/Stabilator Roll

The *Transmission Roll/Stabilator Roll* mode at 14.52526 Hz exhibits limited roll rotation of the transmission structure coupled with the anti-symmetric vertical

bending and yaw rotation of the stabilator (figure 21). This mode is related directly to the previous Stabilator Roll/Transmission Roll mode with minor differences in phase. The fuselage between the midcabin and transition sections undergoes minor roll. Minor lateral bending is found about the aft tailcone section. A 1.5426 % difference from 14.30409 Hz is achieved through the secondary additions. No similar mode is found in modal test.

2nd Vertical Bending/Transmission Vertical

At 14.94383 Hz, the *2nd Vertical Bending/Transmission Vertical* mode is defined on the basis of the well pronounced vertical bending of the full fuselage (figure 22). Uniform vertical translation of the transmission structure and main rotor hub is found. It is noted that very little lateral and longitudinal bending is present with the exception of the tail rotor pylon undergoing longitudinal translation and bending. Anti-symmetric vertical bending and yaw rotation of stabilator is exhibited. A 5.4494 % improvement is achieved from the previous estimate of 14.17157 Hz.

Cockpit/Cabin Roll

The Cockpit/Cabin Roll mode at 17.34857 Hz is characterized by an apparent roll of the cockpit and cabin regions (figure 23). Prominent lateral bending in tailcone section coupled with a roll rotation of the tail rotor pylon base is present. Isolated lateral displacements in nose also occur. Minor yaw rotations in the stabilator including anti-symmetric bending. A 1.7694 percent difference from 17.04694 Hz is achieved with the addition of secondary components.

Stabilator Vertical Bending

The *Stabilator Vertical Bending* mode at 26.84547 Hz is characterized solely by the isolated and well defined symmetric vertical bending of the stabilator wing (figure 24). Small deflections are present in the cockpit window support frames. Minor vertical bending is also exhibited in the tail rotor pylon fold region. A .6555 % difference in frequency from the previous estimate of 27.0226 Hz is achieved with

the addition of secondary components. The *Stabilator Vertical Bending* mode is the last shape found in common among NASTRAN analyses and ground vibration test results.

PRIMARY STRUCTURAL SYSTEM VS. PRIMARY/SECONDARY SYSTEMS

A direct comparison of the two analytical FE models is depicted in Table VI. The first 20 modes of the primary and secondary structural systems are shown to correlate well with primary structural modes. At higher frequencies above 17 Hz, these two analytical models begin to show a greater separation in terms of mode shape frequencies. Table VI shows the mode frequencies of the primary/secondary structural system and the primary structural modes found in common. 'Extra' modes of the primary structural system are found at the following frequencies:

Frequency (Hz)
14.62367
14.71011
19.28929
22.95044
23.10861
24.36330
28.87464
29.07011
34.85303

In the 0 to 35 Hz range, 41 primary structural modes are found in comparison to the 38 modes found for the primary/secondary system. Various forms of stabilator activity are present in all primary structural modes as in the primary/secondary system.

TRENDS & OBSERVATIONS

Additional secondary structural components and the incorporation of modeling revisions to the transmission shell and stabilator has created several noteworthy trends among mode shapes and resonant frequencies:

Stabilator Bending Modes

The presence of numerous mode shapes including the rotation or bending of the stabilator wing is a distinct feature of the primary/secondary structural system. Even with the inclusion of stiffness upgrades of the stabilator springs in the finite element model, realistic characterization of the inherent non-linear behavior of the stabilator will continually prove to be difficult as demonstrated through past shake tests. Of the total 38 modes, 31 involve some form of stabilator activity. Nine mode shapes include anti-symmetric bending of the stabilator while the 22 include symmetric bending of varying degrees. Anti-symmetric stabilator bending components dominate the 4 to 18 Hz range which is characterized by vertical bending. Symmetric bending forms dominate the higher frequency scale after 18 Hz.

Vertical Bending Modes

Mode shapes utilizing vertical bending components in the 4 to 17 Hz are particularly affected. The *1st Vertical Bending* mode at 5.822593 Hz begins a trend in decreasing percent errors between analytical and test results among vertical modes. The modes following the 1st Vertical Bending mode, the Transmission Pitch/2nd Vertical Bending and 2nd Vertical Bending/Transmission Vertical modes, show percent increases in improvement of 15.4129 % and 5.4494 % with shake test results, respectively. From table VII, one can see the trend in correlation improvement. Conversely, decreases in percent error are attained through the increases in structural stiffness. For this set of modes, frequencies consistently increase to match test results.

Transmission Modes

Several of the mode shapes involve some form of transmission activity. Starting with the Transmission Pitch mode at 11.25406 Hz begins a series of coupled modes including transmission roll rotational and vertical translation components.

Stabilator bending or rotation modes are directly coupled with transmission modes in the 4 to 17 Hz range of interest.

Coupling of Mode Shape Sets

For the primary/secondary structural systems, coupling between sets closely spaced modes shapes is common. Three to as many as 4 modes may share distinct bending or torsion components. An excerpt from the previous tabular description of modes for the primary/secondary system is presented in table VIII to demonstrate one such case. Table V shows five modes describing a 'family' of coupled modes in the 17 to 23 Hz range. The first mode, Cockpit/Cabin Roll at 17.34857 Hz, is defined and followed in the second mode at 19.77792 Hz by a similar mode incorporating a fuselage vertical bending component. The three following modes at 20.2, 21.81, and 22.06 Hz incorporate the major bending and torsion components of the first two 'parent' modes in this range. This type of coupling or relation between neighboring modes is consistently seen throughout the entire frequency range.

CORRELATION WITH GROUND VIBRATION TEST RESULTS

PRIMARY/SECONDARY STRUCTURAL SYSTEMS VS. GVT CONFIGURATION

A comparison of shake test mode frequencies with NASTRAN analytical results is presented in table IX. Two interpretations of raw modal test data have been made through the use of SMS Modal 3 SE software and test/data acquisition software by the Imperial College of Science & Technology. Unlike Imperial College software, SMS Modal 3 SE was able to detect the additional modes generated by the bungee suspension system warranting the inclusion of the bungee system into the enhanced finite element model. Generally, shake test estimates from both programs are very similar. However, both interpretations exhibit minor differences in their ability to estimate several modes. Imperial College software did not detect the Stabilator Roll/Transmission Roll test mode at 13.9 Hz. Modal 3 SE software was also deficient in locating the Stabilator Yaw/Pylon Torsion test mode at 15.3 Hz. (It is noted that the Stabilator Yaw/Pylon Torsion mode was not found through analysis for both structural configurations.) Both test programs were unable to detect a Transmission Roll/Stabilator Roll mode found through analysis at 14.5 Hz.

A comparison of NASTRAN estimates show a consistent increase in mode frequencies between the primary structural configuration and primary/secondary system model. These increases offer an improved correlation with shake test estimates. The Stabilator Vertical Bending test mode at approximately 26 Hz is an exception to this general trend by incurring an increase in percent error from a primary structure estimate of 26.85 Hz to the primary/secondary system estimate of 27.02 Hz. Analytical modes correlate well with shake test results below the 4/rev blade passage frequency (17.2 Hz). After this frequency however, correlations show increasing differences as seen in the comparison of test and analytical frequencies for the Cockpit/Cabin Roll and Stabilator Vertical Bending modes.

NON-MATCHING MODES

Several non-matching modes are found in both analysis and test. NASTRAN predictions are able to find the majority of mode shapes with a good estimation of the

resonant frequencies up to 17 Hz. NASTRAN analysis also predicts the relatively distant Stabilator Vertical Bending mode at 26.9 Hz. Between the 17 Hz analysis confidence limit and this distant mode, 11 extra non-matching modes are found as are 8 extra modes above the Stabilator Vertical Bending mode in the 0 to 35 Hz range of interest. Ground vibration test results have also shown the existence of additional mode shapes that could not be adequately defined for the given excitation levels, orientations, and limited number of accelerometer measurements. Of these additional test modes, four are found between the 17 Hz test confidence limit and Stabilator Vertical Bending test mode at 26.1 Hz. Seven additional test modes are found above the Stabilator Vertical Bending test mode. The placement of these undefined deformation states are similar to analysis. It is conceivable that several of these test modes may have already been predicted by NASTRAN analysis. These higher modes may later be defined through an in-house shake test of the current UH-60A Rotor Airloads flight test configuration. It is valuable to note that, unlike most conservative structural analyses (i.e. civil structures) in which the first few modes concerned with structural stability are most important, a rotorcraft study must eventually address higher modal frequencies at discrete regions such as 4/rev and 8/rev blade passage frequencies. One notes that this type of divergence trend at higher frequency correlation is consistent with previous DAMVIBS efforts.

DEVELOPMENT OF VISUALIZATION TOOLS

Graphics software tools are currently being developed by the authors and Glenn Deardorff of the NASA-Ames Computer Systems and Research Division to permit the graphical visualization the UH-60A structural model characteristics. The software is created for the Branch Silicon Graphics Workstation for the graphics post-processing of static characteristic plots such as stress concentration redistributions and the animation of NASA/AEFA analytical mode shapes. Figures 25 and 26 show the visualization of the aerodynamic flow fields about the UH-60A main rotor and fuselage. Figure 27 shows one frame of an animation sequence depicting the deflections occuring in the 1st Lateral Bending mode.

CONCLUSIONS

SECONDARY STRUCTURAL COMPONENTS

The premise of a secondary components study poses *structural stiffness modeling* as the chief cause of discrepancies between GVT results and analytical models. Consistently improved correlations in the lower frequency range show this to be a valid assumption. The discrepancies at higher frequency modes need to be continually addressed however. Although this study is limited in scope and may be configuration dependent, the addition of such components are found to generally improve eigensolution correlations.

A review of the cumulative effects of secondary structure as one gradually compares the primary structural model to a full-up analytical primary/secondary structural system shows that all secondary components must act *in concert* to achieve a *systematic* improvement in mode frequency correlation. The addition of secondary components should be viewed as *one* factor in achieving better correlations.

DAMPING MODEL

The development of an analytical damping model that may be incorporated into a general rotorcraft finite element model may prove useful in addressing the uncorrelated higher frequency modes. In an assessment of issues that needed to be addressed upon the 1989 review of DAMVIBS accomplishments, R. Kvaternik of NASA Langley Research Center cited damping as a one critical area of study for the further development and improvement of vibration predictive models.

Several damping models have been suggested in other areas of study (ie. large flexible space structures). Numerous investigations have been performed to understand several damping mechanisms, accounting for molecular, magnetic, plastic yielding, thermal, and fluid effects. However, the studies were limited in scope to warrant only the support of the individual thesis. No general effort has been conducted to summarize the research results into a wider scoped quantification of the general damping concept. These recent studies were of a varying nature from

diverse disciplines ranging from the study of continuum mechanics to large space structures and optics. Clearly, a great differentiation exists between classifications of damping such as structural or hysteretical, viscous, viscoelastic, material, thermal, proportional, and nonproportional. The individual effects of various sources of damping may eventually be characterized, and their level of participation isolated in terms of its contribution to overall rotorcraft damping. These damping sources could be quantitatively and qualitatively researched encouraging the development of an analytical damping model.

UH-60A AIRLOADS PROGRAM FLIGHT TEST CONFIGURATION

The previous ground vibration tests conducted for the UH-60A configurations under the DAMVIBS and MTRA Program give numerous lessons which may be passed onto planned shake tests of the UH-60A Airloads Program Flight Test Configuration. Among the issues to be addressed are the:

Use of the secondary excitation location at the tail rotor
Assessment of non-linearities and residual terms
Selection of forcing frequencies and applied load magnitudes
Orientation of applied loads
Determination of applied loads
Selection of suspension system and determination of its error contribution
Selection of data acquisition and interpretation hardware and software
Practical placement of measurement locations

These test concepts must be defined in the pre-shake test phase. The descriptions and results from previous UH-60A tests will serve as an invaluable experience base for future tests.

RECOMMENDATIONS

REVIEW OF AVAILABLE OPTIMIZATION TECHNIQUES

A review of potential optimization techniques should be conducted for the continuation of model refinement. Accurate results from the planned shake test of the UH-60A Airloads Program Flight Test Configuration will prove valuable in ascertaining the types of modifications that should be made. This is reasonable since many optimization codes must use some form of modal test data as a reference database from which to improve correlations. For the UH-60A NASTRAN model, three current methods appear viable:

1) **PAREDYM** PArametric REfinement of DYnamic Models
   A nonlinear programming code by Sikorsky and the University of Bridgeport

2) **NASTRAN**
   Recently developed formats for Design Sensitivity and Optimization analyses

3) **COPES/CONMIN**
   System Identification/Optimization routines developed by NASA and H. Miura

Clearly, the continuing refinement of the UH-60A is becoming increasingly dependent upon the use of optimization and system identification applications/disciplines.

VISUALIZATION METHODS

Discussions and collaborative work regarding Visualization techniques should be continued with Glenn Deardorff of the Computer Systems and Research Division. The development of a generic NASTRAN graphics post-processor for purposes of dynamic mode shape identification and video presentation of the UH-60A Model should be completed before the planned shake test. The post-processor will allow a more time efficient analysis of static characteristics to be made through the use of contouring, color graphics, and other visualization benefits. Although other post-processors are available in the commercial market (ie. PATRAN), use of the graphics

software on the Silicon Graphics Workstation will prove superior in terms of video presentation material.

UH-60A AIRLOADS PROGRAM REVIEW COMMITTEE RECOMMENDATION

Based upon the recommendations of the UH-60A Airloads Program Review Committee, which met with members of the Rotorcraft Flight Technology, Flight Experiments, and Rotorcraft Aeromechanics Branches in May 1990, work for a NASTRAN remodeling effort is proposed. The committee, including engineers and faculty from both industry and academia, suggests that a vibration survey of the UH-60A flight test airframe be included as a complementary component of the continuing UH-60A flight test program. It was shown that in-flight vibration test data would be of minimal use unless a parallel commitment were made to a complete ground vibration test and modal analysis with accompanying finite element analysis of the flight test airframe configuration.

ADDITIONAL MODELING OF FLIGHT COMPONENTS

The current structural configuration of the UH-60A flight test craft is shown in figure 28. This unique article is similar to the previously described NASA/AEFA GVT and NASTRAN configurations. This flight test article however, in addition to flight masses, will carry the corresponding true flight components such as instrumentation racks, ballast rack, ballast cart, etc. Previous GVT and NASTRAN analyses have reflected changes in mass distribution only. No changes in stiffness due to these flight components have been considered since they were not included in NASA/AEFA shake tests. Extra flight instrument components such as instrumentation booms have also been added since the NASA/AEFA GVT. The following is a list of flight members contributing mass *and* structural stiffness to the UH-60A flight configuration:

MUX Instrumentation Bucket
Ballast Rack
Movable Ballast Cart
Instrumentation Racks (4)

Power Source/Converter Mount
Laser Cube Mounts (2)
Instrument Bar
Instrument Boom
Formatter/Multiplexer Mount
Multiplexer Base
Observer Station Mount and Seat
Tape Recorder Mount
Various Instrumentation Boxes

A few of these components may be deemed insignificant in contributing stiffness or mass to the model (ie. laser cube mount). But most of these items will contribute a notable difference in dynamic response, particularly on the cabin floor where a full ballast rack, ballast cart, and five instrument mounts will locally increase stiffness. The role of other members in changing global dynamic response, such as the instrument boom and bar, need to be ascertained. Both these members are mounted directly to frames and longitudinal beams in the forward cabin and cockpit. A majority of these members may be added to the existing finite element model through the use of approximations or full substructures to reflect their suitable stiffness and mass effects. A corresponding shake test of the full UH-60A flight test helicopter is planned within the next two years for the eventual correlation of frequency and time domain data.

TABLE I

NASA/AEFA GVT Excitation Levels & Frequency Ranges

Excitation Location	Frequency Range	Force Level
Main Rotor Hub Vertical	3 to 45 Hz	±100 - 200 lbs
Main Rotor Hub Lateral	3 to 40 Hz	±100 - 200 lbs
Main Rotor Hub Longitudinal	3 to 40 Hz	±100 - 200 lbs
Tail Pylon Vertical	3 to 40 Hz	Variable
Tail Pylon Lateral	3 to 40 Hz	Variable

TABLE II

CABIN DOOR STIFFNESS APPROXIMATIONS

Frequency Comparison for DAMVIBS baseline UH-60A: Decreasing % errors

		Frequency (Hz)	
Mode Description	Test	NASTRAN / %error (without cabin doors)	NASTRAN / %error (with cabin doors)
Second Vertical Bending	14.01	12.4 / 12%	13.5 / 3.6%
Third Vertical Bending	19.36	18.1 / 7%	19.8 / 2.6%

TABLE III

RIGID BODY CHECK/ENFORCED DISPLACEMENT OUTPUT
'Excerpt from Printed Output'

D I S P L A C E M E N T V E C T O R

POINT ID.	TYPE	T1	T2	T3	R1	R2	R3
2531	G	-9.999993E-01	1.843909E-09	-4.194581E-07	-6.273021E-12	-7.315051E-09	4.242626E-12
2533	G	-9.999993E-01	1.829559E-09	-4.195052E-07	-1.464132E-11	-7.313072E-09	1.867273E-11
2534	G	-9.999993E-01	1.906437E-09	-4.194486E-07	-1.652777E-11	-7.333439E-09	7.027879E-12
2535	G	-9.999994E-01	2.062021E-09	-4.193898E-07	-3.205319E-11	-7.357449E-09	3.655108E-11
2536	G	-9.999994E-01	2.237121E-09	-4.193437E-07	-4.663989E-11	-7.346390E-09	5.606718E-11
2537	G	-9.999995E-01	2.614731E-09	-4.192902E-07	-5.080231E-11	-7.354289E-09	7.562560E-11
2538	G	-9.999995E-01	2.929490E-09	-4.192610E-07	-6.029688E-11	-7.337942E-09	9.639514E-11
2543	G	-9.999997E-01	2.121393E-09	-4.261821E-07	3.762904E-10	-7.404110E-09	-4.457687E-11
2544	G	-9.999998E-01	6.674328E-10	-4.243097E-07	3.985719E-10	-7.402421E-09	2.083921E-11
2545	G	-9.999998E-01	1.494967E-10	-4.220117E-07	3.952850E-10	-7.369316E-09	-4.794650E-11
2546	G	-9.999998E-01	-3.319056E-10	-4.194091E-07	3.506480E-10	-7.338067E-09	2.857024E-11
2547	G	-9.999998E-01	-4.362239E-10	-4.174445E-07	2.598342E-10	-7.199496E-09	2.741126E-11
2548	G	-9.999998E-01	-1.884627E-10	-4.162764E-07	1.565624E-10	-7.469614E-09	-1.285486E-11
2549	G	-9.999998E-01	7.317303E-14	-4.155699E-07	7.474716E-11	-7.659618E-09	7.628036E-12
2580	G	-9.999993E-01	1.894557E-09	-4.195199E-07	0.0	0.0	0.0
2582	G	-9.999993E-01	1.881496E-09	-4.194563E-07	0.0	0.0	0.0
2583	G	-9.999993E-01	1.875301E-09	-4.194713E-07	0.0	0.0	0.0
2584	G	-9.999993E-01	1.856366E-09	-4.194441E-07	0.0	0.0	0.0
2586	G	-9.999993E-01	1.834586E-09	-4.193792E-07	0.0	0.0	0.0
2587	G	-9.999993E-01	1.801581E-09	0.0	0.0	0.0	0.0
2590	G	-9.999993E-01	1.766603E-09	0.0	0.0	0.0	0.0
2591	G	-9.999993E-01	1.733208E-09	-4.189397E-07	0.0	0.0	0.0
2593	G	-9.999993E-01	1.710687E-09	-4.186985E-07	0.0	0.0	0.0
2594	G	-9.999993E-01	1.690717E-09	-4.184030E-07	0.0	0.0	0.0
2596	G	-9.999993E-01	1.683684E-09	-4.180936E-07	0.0	0.0	0.0
2597	G	-9.999993E-01	1.669326E-09	-4.178557E-07	0.0	0.0	0.0
2601	G	-9.999998E-01	1.574726E-10	-4.153305E-07	-9.875194E-12	-7.648250E-09	1.211921E-10
2602	G	-9.999998E-01	-7.671498E-12	-4.156502E-07	-9.505627E-11	-7.369642E-09	2.740651E-10
2603	G	-9.999998E-01	-2.133126E-10	-4.165990E-07	-2.090327E-10	-7.071729E-09	1.579859E-10
2604	G	-9.999998E-01	-6.194700E-10	-4.180181E-07	-3.133643E-10	-7.183414E-09	-2.142892E-10
2605	G	-9.999998E-01	-1.193469E-09	-4.203450E-07	-3.534826E-10	-7.393227E-09	-1.300910E-11
2606	G	-9.999997E-01	-1.584604E-09	-4.223729E-07	-3.347312E-10	-7.420058E-09	2.619176E-11

Constraints to be checked

Unit Displacements

Negligible translation/rotations (zero)

TABLE IV

Changes in Mode Frequencies from Secondary Structural Components

Cumulative Breakdown of Components from Analytical Full-Up Structure

	Full Structure	-Gunner Windows	-Cabin Doors	-Cockpit Windshields	-Cockpit Doors	-Firewall	-Xssn Support	-Xssn Shell Property
1st Lateral Bending	4.988069	4.98804	4.965894	4.954474	4.954414	4.946419	4.946352	4.944847
1st Vertical Bending	6.544949	6.525377	6.047724	6.03784	6.004512	5.82829	5.827287	5.822593
Stabilator Roll	10.06609	10.06456	9.956318	9.941495	9.936351	9.881579	9.880489	9.866302
Transmission Pitch	13.33652	12.97417	11.25406	11.25247	11.24942	10.55532	10.53568	10.4672
Transmission Pitch/2nd Vertical Bending	14.34413	14.26024	13.07353	12.60329	11.4441	11.42817	11.4027	11.32761
Transmission Roll/Stabilator Yaw	13.82205	13.76387	13.75396	13.70139	13.69304	13.44995	13.69163	13.68203
Stabilator Roll/Transmission Roll	14.57081	14.56853	14.14592	14.12703	14.12976	13.89309	13.3354	13.033
Transmission Roll/Stabilator Roll	15.35103	15.32258	14.52526	14.33936	14.32018	14.30964	14.307	14.30409
2nd Vertical Bending/Transmission Vertical	17.96042	17.69793	14.94383	14.93157	14.91054	14.61316	14.60164	14.17157

TABLE V

MODAL FREQUENCY / SHAPE

UH-60A Primary & Secondary Structural Systems
NASA/AEFA Weight Distribution

MODE NO.	FREQ. (Hz)	MODE DESCRIPTION	COMMENTS
1	.001338	Rigid Body	Uniform roll centered about longitudinal axis .
2	.001421	Rigid Body	Longitudinal translation with slight roll.
3	.001546	Rigid Body	Uniform yaw rotation about transition section. Lateral Lateral displacements dominate with slight roll.
4	.001585	Rigid Body	Lateral translation with slight roll about longitudinal axis.
5	1.242446	Rigid Body	Uniform pitch rotation about aft cabin area. Vertical displacements dominate. Significant displacement in tailcone transition section to pylon areas.
6	1.324921	Rigid Body	Vertical translation.
7	4.965894	1st Lateral Bending	Lateral movement. Anti-symmetric bending w/ Torsion and yaw in stabilator. Significant torsion in tail rotor pylon starting at pylon fold joint.

8	6.047724	1st Vertical Bending	Vertical bending centered about midcabin section. Vertical displacements in stabilator due to upward movement of tail rotor pylon base at fold joint.
9	9.956318	Stabilator Roll	Characterized by isolated anti-symmetric bending of stabilator. Anti-symmetric bending of stabilator. Minor lateral bending in aft tailcone before fold joint.
10	11.25406	Transmission Pitch	Mode shape characterized by pitching of transmission section and main rotor hub shaft. Significant vertical bending in tailcone with anti-symmetric bending of stabilator. Longitudinal displacements found in tail rotor pylon. Limited vertical bending in cabin areas.
11	13.07353	Transmission Pitch/ 2nd Vertical Bending	Notable vertical displacements in nose,cockpit/cabin transition section to transition section,tailcone, with anti-symmetric vertical and yaw bending of stabilator. Pitching of transmission shaft. Vertical bending of general tailcone section. Well defined vertical bending of fuselage.
12	13.75396	Transmission Roll/ Stabilator Yaw	Stabilator roll/yaw from anti-symmetric bending. Isolated and limited vertical/lateral displacements near nose and tailcone aft. Limited transmission roll.
13	14.14592	Stabilator Roll/ Transmission Roll	Vertical displacements in cockpit and tailcone regions. Significant displacements due to roll found in main rotor hub and transmission support structure. Anti-symmetric roll bending w/ yaw rotation of stabilator. Minor vertical bending displacements on midcabin floor from rolling of transmission.
14	14.52526	Transmission Roll/ Stabilator Roll	Anti-symmetric vertical bending and yaw rotation in stabilator. Midcabin to transition section undergoes minor roll. Minor lateral bending about aft tailcone section.
15	14.94383	2nd Vertical Bending/ Transmission Vertical	Anti-symmetric vertical bending and yaw rotation of stabilator. Well defined vertical bending of full fuselage. Very little lateral and longitudinal bending with exception of tail rotor pylon undergoing longitudinal translation and bending. Uniform

			vertical displacement translation of transmission structure and main rotor hub.
16	15.54864	2nd Vertical Bending/ Transmission Pitch	Distinct vertical bending of global fuselage coupled with pitching and vertical bending of transmission. Symmetric bending of stabilator with limited yaw rotation.
17	17.34857	Cockpit/Cabin Roll	Apparent roll in cockpit and cabin regions. Prominent lateral bending in tailcone section coupled with roll rotation of TR pylon base. Isolated lateral displacements in nose. Minor yaw rotation in stabilator including anti-symmetric bending.
18	19.77792	3rd Vertical Bending/ Cockpit/Cabin Torsion	Two significant vertical bending components about cockpit and aft cabin section. Minor lateral bending in forward tailcone. Significant deformation in nose, forward cabin, & rear cabin/transition including vertical compression of frames in forward cabin/aft cockpit. Limited transmission pitch and yaw. Symmetric bending in stabilator with tail rotor pylon pitch.
19	20.20211	3rd Vertical Bending	Well pronounced vertical bending of fuselage including displacements in cockpit, cabin, and transition section. Defined vertical bending of tailcone region and tail rotor pylon. Symmetric bending of stabilator.
20	21.81364	Cockpit/Cabin Roll / 3rd Vertical Bending	Roll of cockpit, forward and aft cabin areas coupled with vertical bending of tailcone and aft transition section. Symmetric bending of stabilator.
21	22.06097	Transmission Pitch/ Cockpit/Cabin Roll / 3rd Vertical Bending	Possible coupling of modes 19 and 20 with pitching of transmission structure and main rotor hub. Global vertical bending of fuselage in cockpit, cabin and tailcone regions. Symmetric bending of stabilator.
22	22.74920	Cockpit Vertical/ Stabilator Bending	Isolated vertical bending in cockpit and forward cabin regions. Minor vertical displacement in forward tailcone area. Symmetric bending of stabilator.
23	23.00699	Cockpit Vertical I	Mode closely resembles mode 22 with isolated vertical bending in cockpit and forward cabin. Small bending in aft transition

			section. Very minor symmetric and vertical stabilator bending. Landing gear support struts undergo outward lateral displacements.
24	23.07595	4th Vertical Bending	Fuselage vertical bending in cockpit, cabin, transition, and tailcone sections. *Minor pitching of transmission structure and main rotor hub.* Symmetric bending of stabilator. Outward lateral displacements of landing gear struts.
25	23.74587	Transmission Pitch/ 4th Vertical Bending	Mode closely related to previous mode. Full fuselage vertical bending with greater definition of transmission structure pitch. Cabin rolling introduced. Symmetric bending of stabilator.
26	24.03611	Cabin Torsion	Well defined torsion of cockpit, cabin, transition sections with minor vertical translation of tailcone. Symmetric bending of stabilator. Minor pitching of transmission.
27	24.54303	Transmission Pitch/ Cabin Torsion	Torsion of cockpit, cabin, transition sections. Uniform torsion of tailcone regions. Greater definition of pitch and yaw rotation of transmission than previous mode. Symmetric bending of stabilator.
28	25.94303	Stabilator Vertical Bending/ Transmission Pitch	Symmetric vertical bending of stabilator with pitch rotation of transmission and main rotor hub shaft. Minor vertical displacements in cockpit, top aft transition section, and tailcone.
29	26.84547	Stabilator Vertical Bending	Mode characterized solely by isolated and well pronounced symmetric vertical bending of stabilator. Small displacement in cockpit window support frames. Minor vertical bending in tail rotor pylon fold region.
30	28.20623	Forward Cabin Bending	Vertical bending centered about forward cabin section. Minor vertical bending in aft transition section and tailcone. Symmetric stabilator bending present. Longitudinal translation.
31	28.82991	Transmission Yaw/ 2nd Lateral Bending	Pitch rotation of transmission structure. Vertical and lateral bending of fuselage. Lateral bending of fuselage with tailcone predominant. *Torsion/roll of cockpit section.* Symmetric vertical

			bending and yaw rotation of stabilator. Bending of tail rotor pylon.
32	29.98946	Forward Cabin Torsion	Torsion/roll of cockpit and forward cabin becomes more pronounced. *Transmission yaw rotation* present with symmetric vertical bending of stabilator. Minor *lateral bending of tailcone* still present.
33	30.27442	5th Vertical Bending	Vertical bending of forward fuselage with emphasis of bending in forward cabin. Bending also present in cockpit and aft cabin section. Tailcone show uniform bending with lateral displacement. Symmetric bending of stabilator. *Transmission yaw rotation still present.*
34	30.53515	Cabin Compression/ Vertical Bending	Vertical compression of aft cockpit and forward cabin frames. 5th *Vertical bending of tailcone* with similar lateral bending component. Midcabin undergoes roll rotation. Symmetric vertical bending of stabilator with slight yaw rotation. *Transmission yaw rotation still present.*
35	32.82293	Cockpit Vertical II	Isolated vertical displacements in cockpit nose and cockpit window supports. *Slight cabin floor roll. Slight transmission yaw rotation still present.* Minor symmetric bending of stabilator.
36	33.86091	Cockpit Compression I	Significant bending of frames in aft cockpit and forward cabin. Pitch and roll rotations of transmission structure and main rotor hub shaft. Significant lateral bending of tailcone. Symmetric vertical bending and yaw rotation of stabilator. Bending of tail rotor pylon.
37	34.11718	Cockpit Compression II	Pitch and minor roll rotation of transmission structure. Vertical compression of aft cockpit and forward cabin frames. Midcabin roll. Deflections present in cockpit window supports. Significant bending of transition section floor. Significant lateral bending of tailcone. Full yaw rotation and minor symmetric bending of stabilator.

38	34.66370	Cockpit Compression III	Minor compression of aft cockpit and forward cabin regions. Minor vertical bending components through cockpit and cabin. Pitch and roll rotation of transmission. Minor vertical bending of tailcone. Slight symmetric bending of stabilator with minor yaw rotation.

TABLE VI

Comparison of
Primary Structural System vs. Primary/Secondary Structural Systems
UH-60A NASA/AEFA Weight Distribution

Frequency (Hz) PRIMARY	PRIMARY & SECONDARY	MODE DESCRIPTION
.001340	.001338	Rigid Body
.001354	.001421	Rigid Body
.001437	.001546	Rigid Body
.001597	.001585	Rigid Body
1.240584	1.242446	Rigid Body
1.321255	1.324921	Rigid Body
4.944847	4.965894	1st Lateral Bending
5.822593	6.047724	1st Vertical Bending
9.866302	9.956318	Stabilator Roll
10.46720	11.25406	Transmission Pitch
11.32761	13.07353	Transmission Pitch/2nd Vertical Bending
13.68203	13.75396	Transmission Roll/Stabilator Yaw
13.03300	14.14592	Stabilator Roll/Transmission Roll
14.30409	14.52526	Transmission Roll/Stabilator Roll

14.17157	14.94383	2nd Vertical Bending/Transmission Vertical
15.98261	15.54864	2nd Vertical Bending/Transmission Pitch
17.04964	17.34857	Cockpit/Cabin Roll
17.6118	19.77792	3rd Vertical Bending/Cockpit/Cabin Torsion
20.08978	20.20211	3rd Vertical Bending
21.84601	21.81364	Cockpit/Cabin Roll /3rd Vertical Bending
*	22.06097	Transmission Pitch/ Cockpit/Cabin Roll / 3rd Vertical Bending
22.75370	22.74920	Cockpit Vertical/Stabilator Bending
21.39138	23.00699	Cockpit Vertical I
22.64246	23.07595	4th Vertical Bending
*	23.74587	Transmission Pitch/4th Vertical Bending
23.85199	24.03611	Cabin Torsion
25.54303	24.54303	Transmission Pitch/Cabin Torsion
25.93453	25.94903	Stabilator Vertical Bending/Transmission Pitch
27.02260	26.84547	Stabilator Vertical Bending
*	28.20623	Forward Cabin Bending
30.02654	28.82991	Transmission Yaw/2nd Lateral Bending
30.86615	29.98946	Forward Cabin Torsion
*	30.27442	5th Vertical Bending
*	30.53515	Cabin Compression/5th Vertical Bending
*	32.82293	Cockpit Vertical II
34.45077	33.86091	Cockpit Compression I
32.78901	34.11718	Cockpit Compression II
32.5025	34.66370	Cockpit Compression III

*No mode found similarly in primary/secondary structural systems

TABLE VII

Vertical Bending Modes & Shake Test Results

	Frequency/Percent Error		
Mode Description	Primary	Primary & Secondary	Shake Test
1st Vertical Bending	5.822593 / 7.578%	6.047724 / 4.004%	6.3
Transmission Pitch/2nd Vertical Bending	11.32761 / 12.189%	13.07353 / 1.345%	12.9
2nd Vertical Bending/Transmission Vertical	14.17157 / 1.586%	14.94383 / 3.777%	14.4 (estimation)

TABLE VIII

COUPLING OF MODE SETS
"Excerpt from Mode Descriptions"

UH-60A Primary & Secondary Structural Systems
NASA/AEFA Weight Distribution

FREQ. (Hz)	MODE DESCRIPTION	COMMENTS
17.34857	Cockpit/Cabin Roll	Apparent roll in cockpit and cabin regions. Prominent lateral bending in tailcone section coupled with roll rotation of TR pylon base. Isolated lateral displacements in nose. Minor yaw rotation in stabilator including anti-symmetric bending.
19.77792	3rd Vertical Bending/ Cockpit/Cabin Torsion	Two significant vertical bending components about cockpit and aft cabin section. Minor lateral bending in forward tailcone. Significant deformation in nose, forward cabin, & rear cabin/transition including vertical compression of frames in forward cabin/aft cockpit. Limited transmission pitch and yaw. Symmetric bending in stabilator with tail rotor pylon pitch.
20.20211	3rd Vertical Bending	Well pronounced vertical bending of fuselage including displacements in cockpit, cabin, and transition section. Defined vertical bending of tailcone region and tail rotor pylon. Symmetric bending of stabilator.
21.81364	Cockpit/Cabin Roll / 3rd Vertical Bending	Roll of cockpit, forward and aft cabin areas coupled with vertical bending of tailcone and aft transition section. Symmetric bending of stabilator.

22.06097	Transmission Pitch/ Cockpit/Cabin Roll / 3rd Vertical Bending	Possible coupling of modes 19 and 20 with pitching of transmission structure and main rotor hub. Global vertical bending of fuselage in cockpit, cabin and tailcone regions. Symmetric bending of stabilator.

TABLE IX

COMPARISON OF GROUND VIBRATION RESULTS WITH NASTRAN ANALYSIS
NASA/AEFA Weight Distribution

Mode Description	Shake Test		NASTRAN Model	
	Imperial College	Modal 3 SE	Primary & Secondary	Primary
1st Lateral Bending	5.4	5.4	4.965894	4.944847
1st Vertical Bending	6.3	6.3	6.047724	5.822593
Stabilator Roll	9.9	10.0	9.956318	9.866302
Transmission Pitch	11.6	11.6	11.25406	10.46720
Transmission Pitch/2nd Vertical Bending	13.0	12.9	13.07353	11.32761
Transmission Roll/Stabilator Yaw	13.6	13.5	13.75396	13.68203
Stabilator Roll/Transmission Roll	*	13.9	14.14592	13.03300
Transmission Roll/Stabilator Roll	-	-	14.52526	14.30409
2nd Vertical Bending/Transmission Vertical	14.5	14.4	14.94383	14.17157
Stabilator Yaw/Pylon Torsion	15.3	**	***	***
Cockpit/Cabin Roll	15.8	15.8	17.34857	17.04694
Stabilator Vertical Bending	25.9	26.1	26.84547	27.02260

- Mode not detected in Shake Test.
* Mode not detected with Imperial College Software Analysis.
** Mode not detected with Modal 3 SE Software Analysis.
*** Mode not found in NASTRAN analysis

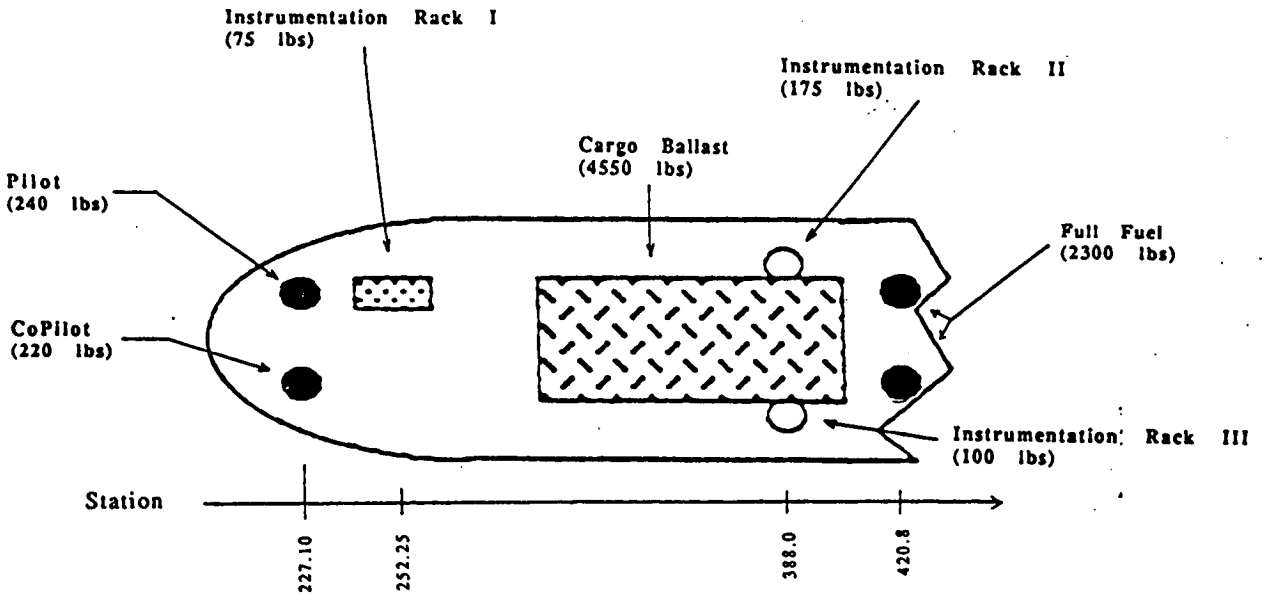

NASA/AEFA WEIGHT DISTRIBUTION

Shake Test Weight

DAMVIBS = 10,140 lbs
NASA/AEFA = 17,800 lbs

Figure 1. NASA/AEFA Test Weight Distribution - NASTRAN & GVT

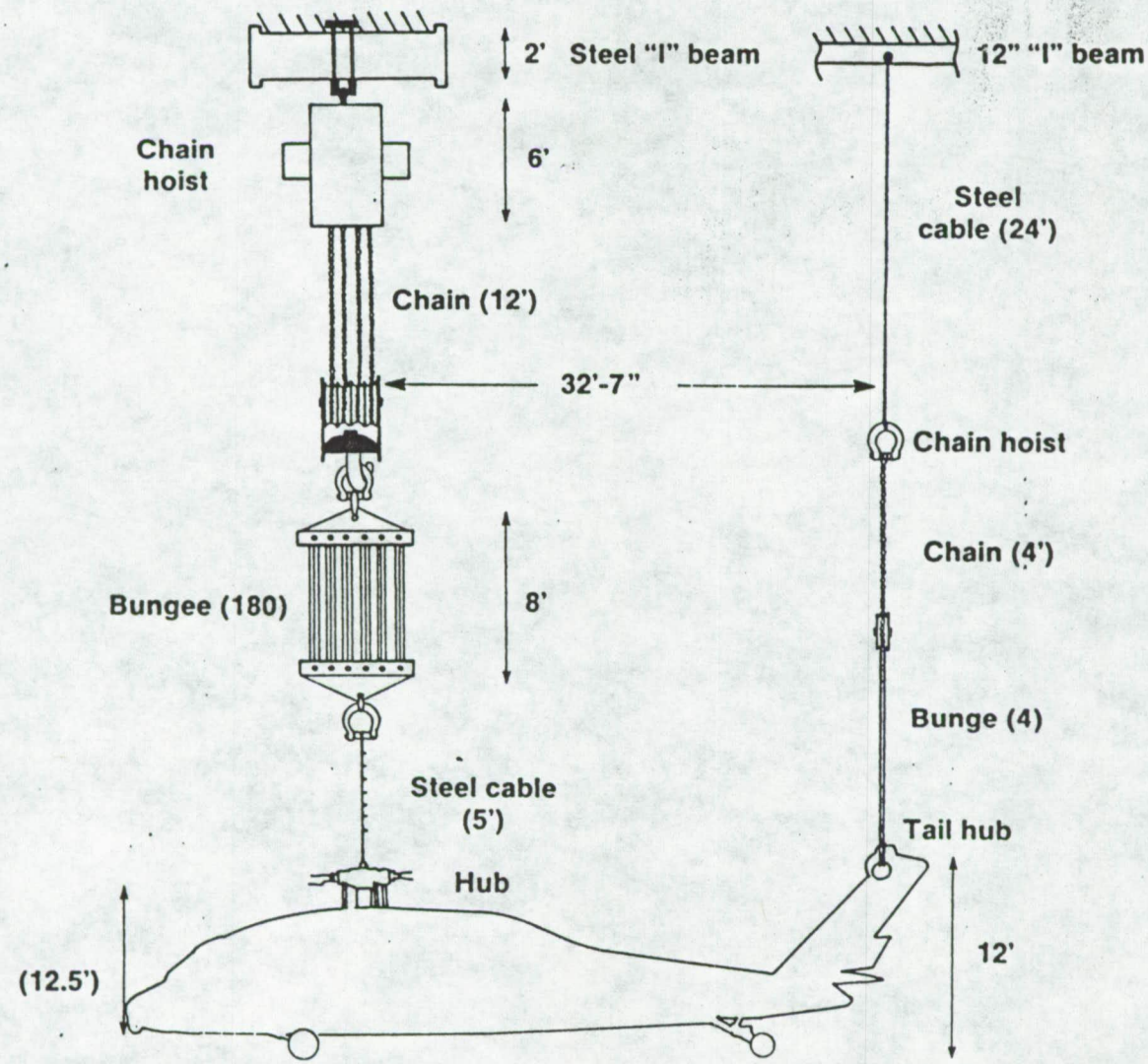

Figure 2. Ground Vibration Test Suspension System Layout

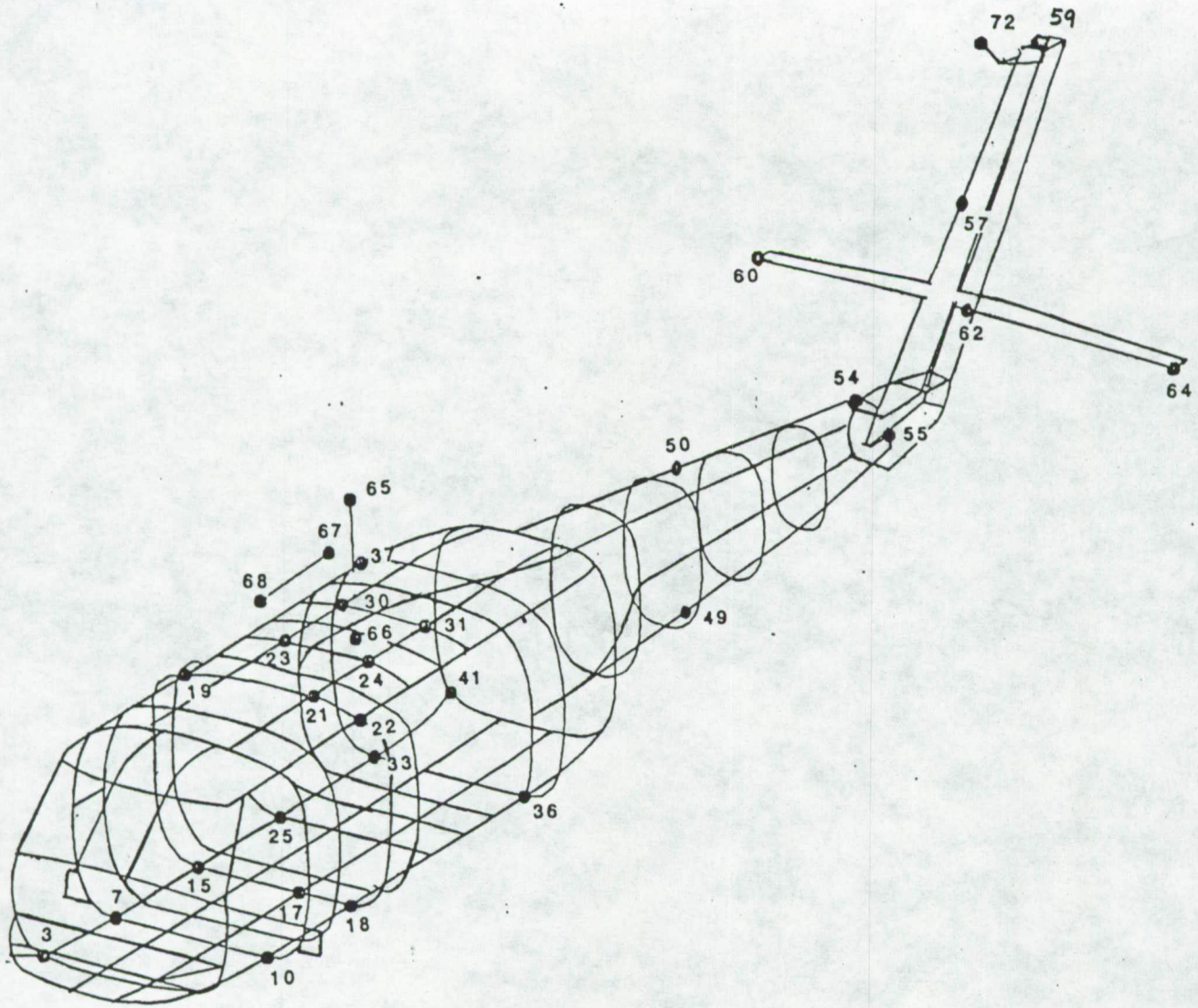

Figure 3. NASA/AEFA GVT Measurement Locations

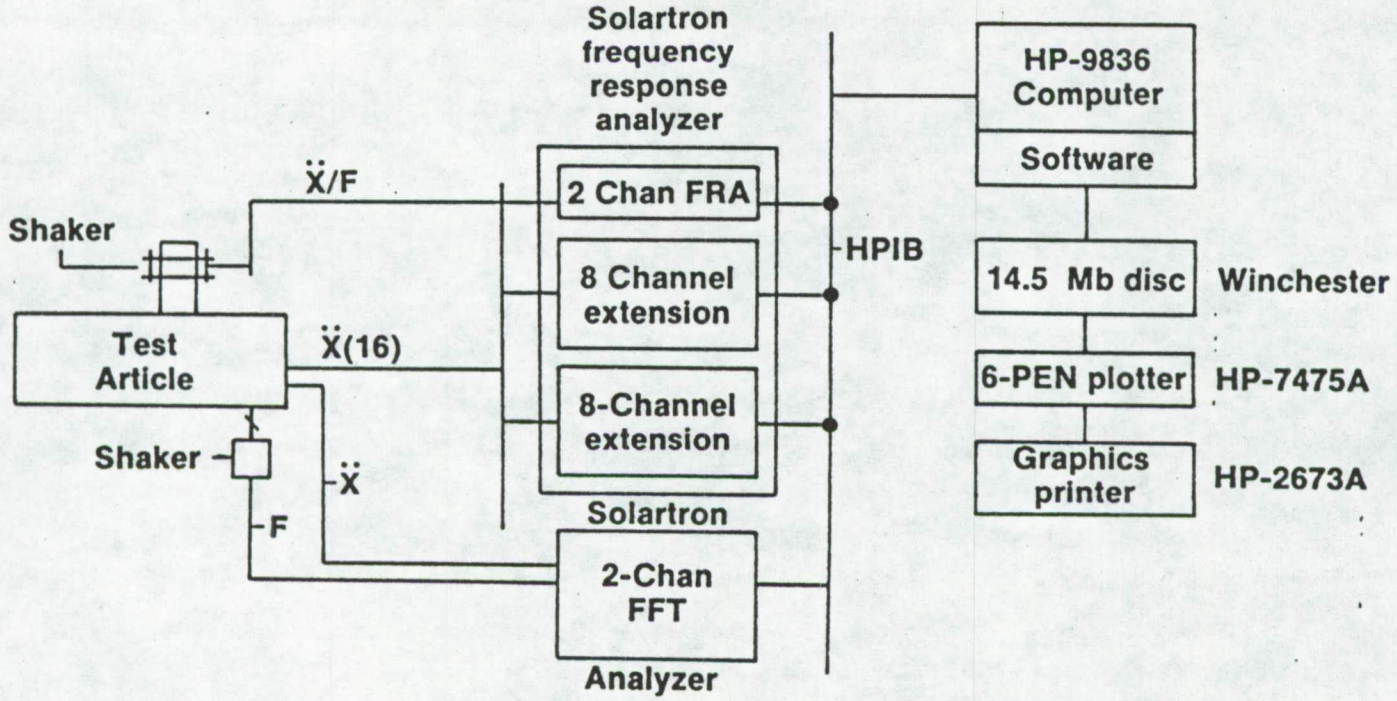

Figure 4. GVT Data Acquisition & Analysis System

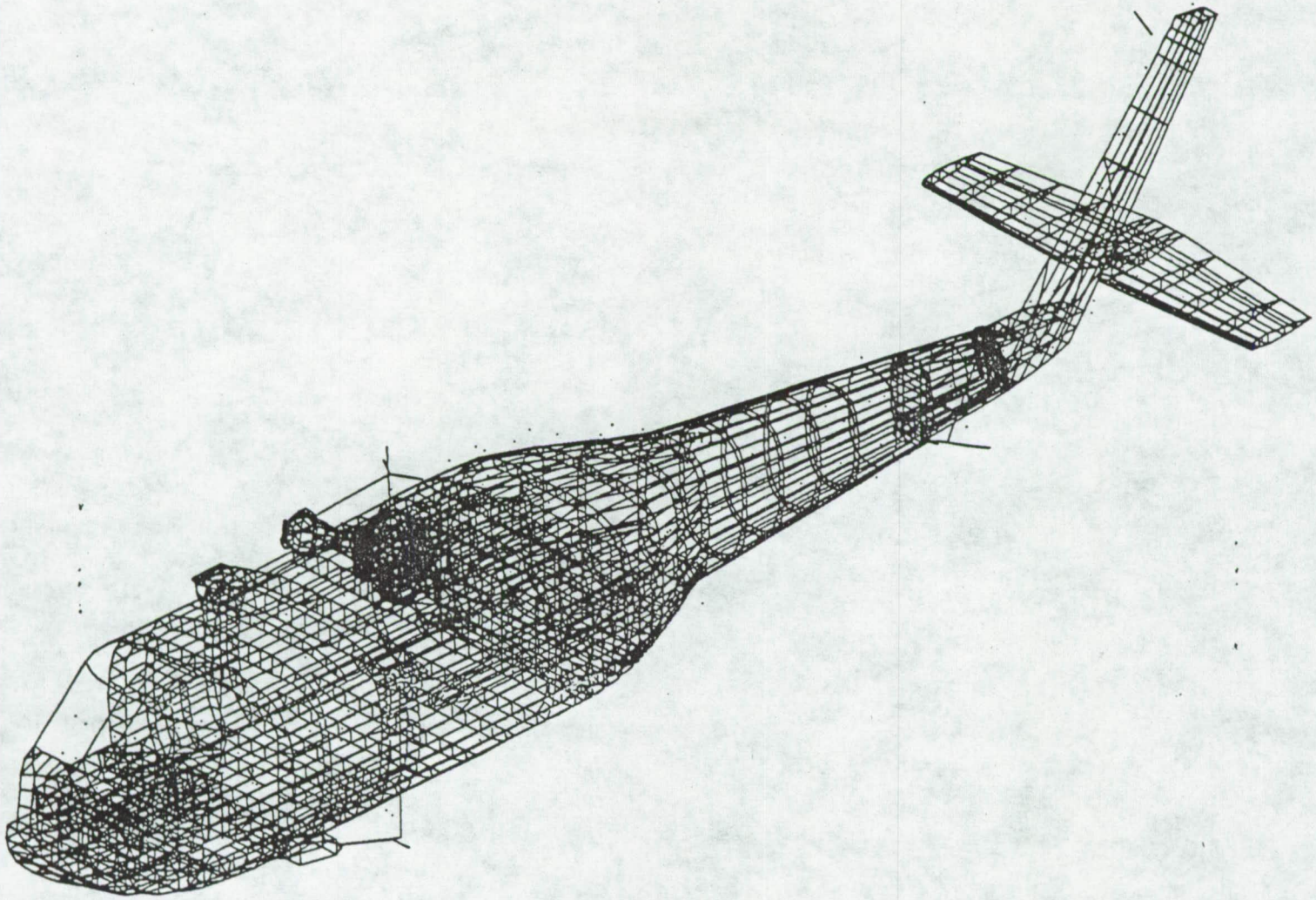

Figure 5. NASTRAN Primary Structural System

Secondary Structural Components

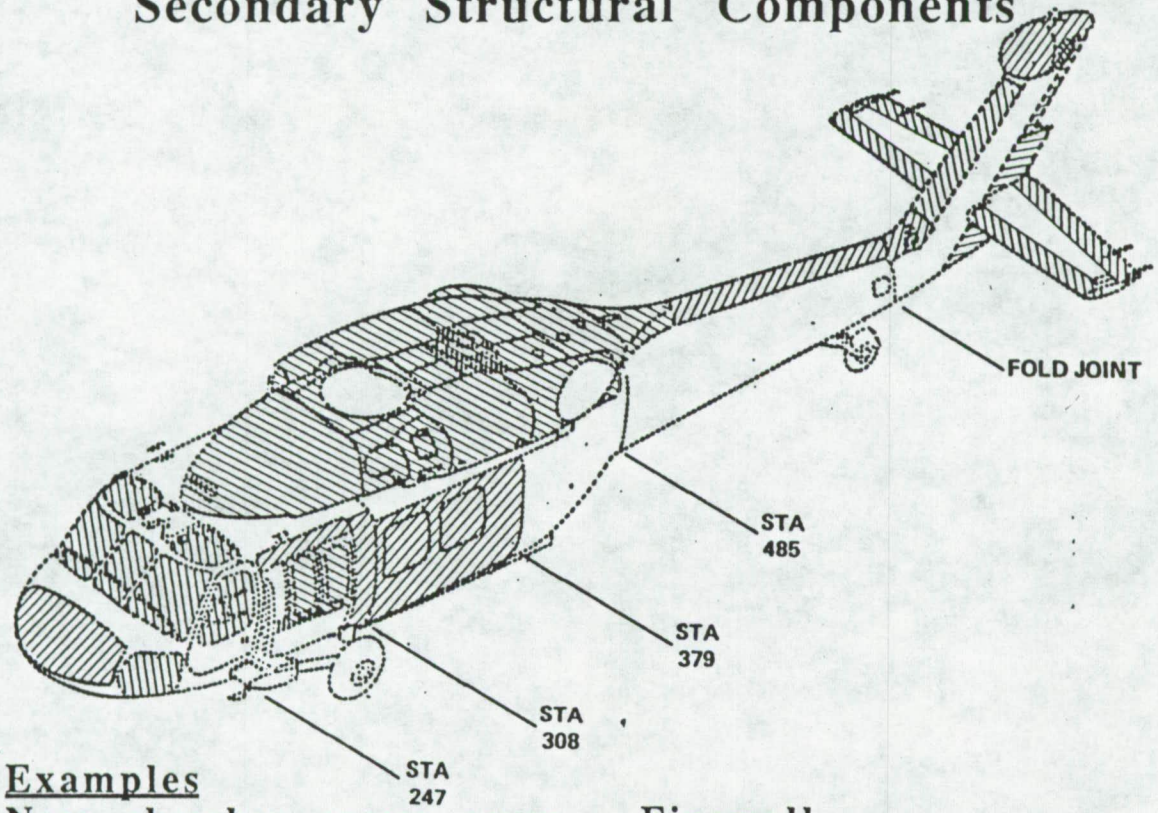

Examples

Nose absorber access cover
Cockpit Windows
Cockpit Doors
Gunner Windows
Lower Pylon Fairings
Cabin Doors
Firewall
Transmission Bridge
Tail gearbox covers
Various TR Pylon fairings
Various stabilator fairings

Figure 6. Examples of Typical Secondary Structural Components

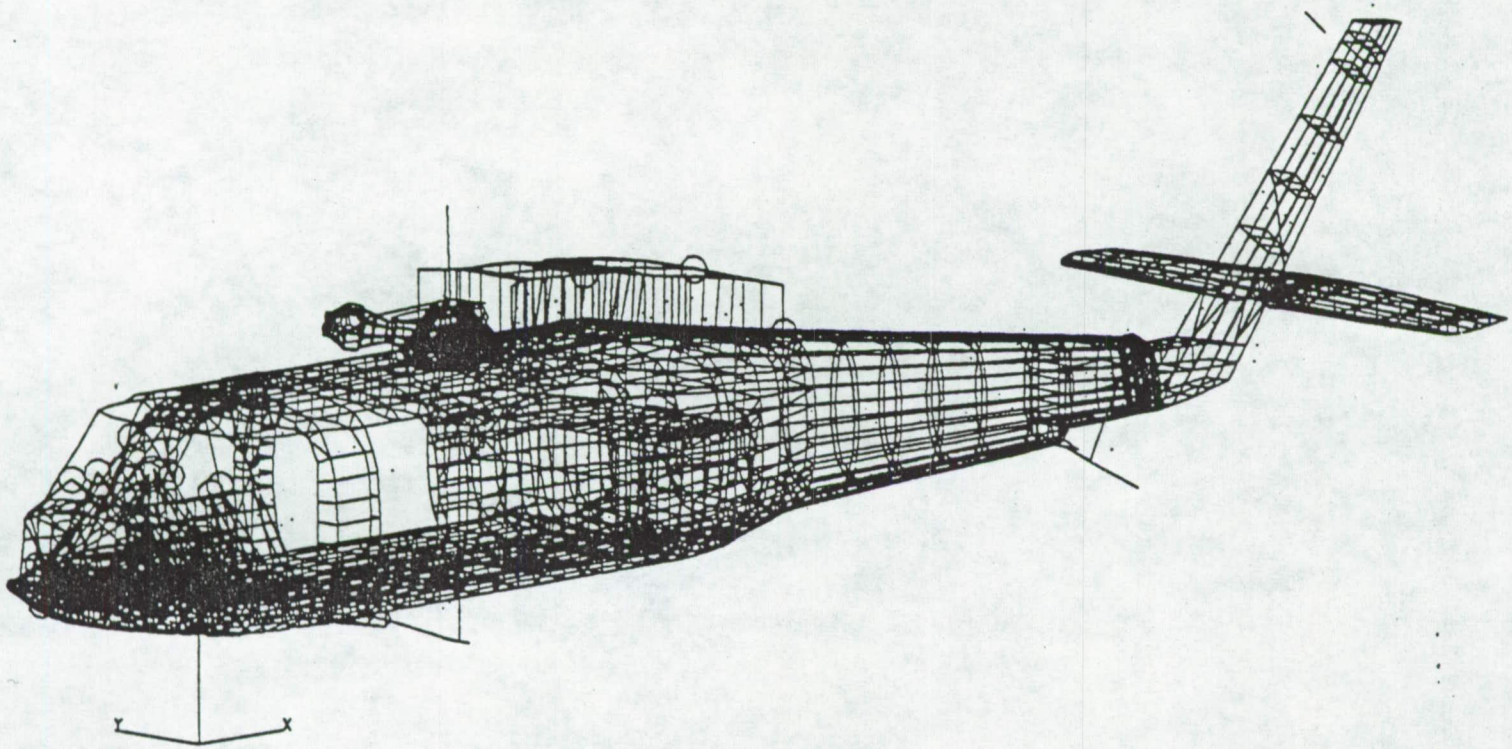

Figure 7. NASTRAN Primary & Secondary Structural Systems

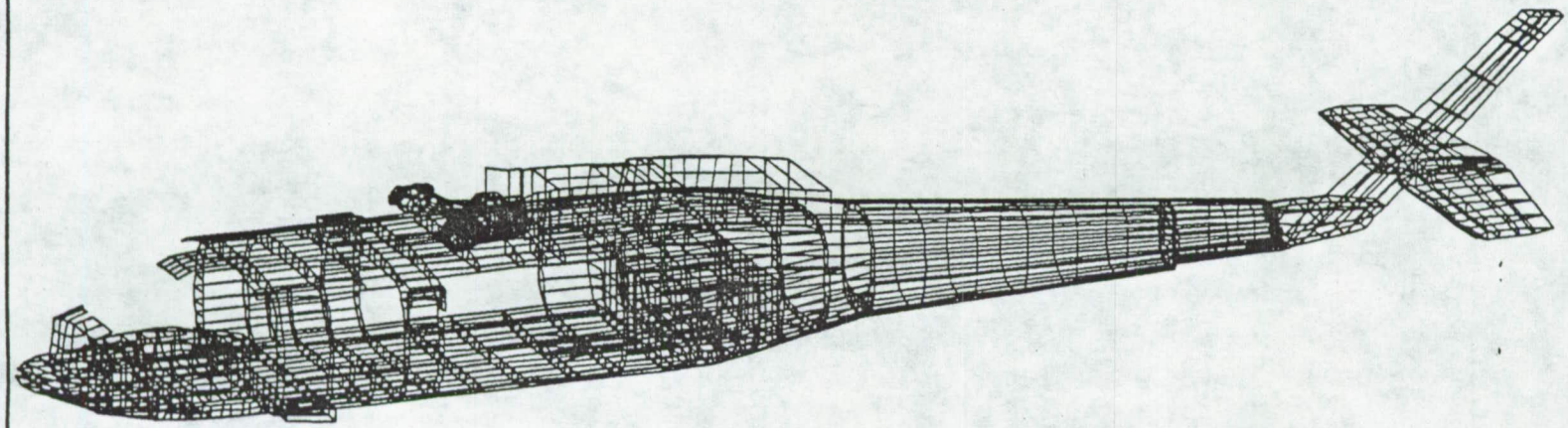

Figure 8. UH-60A Primary/Secondary Structure Model: CQUAD4 Elements

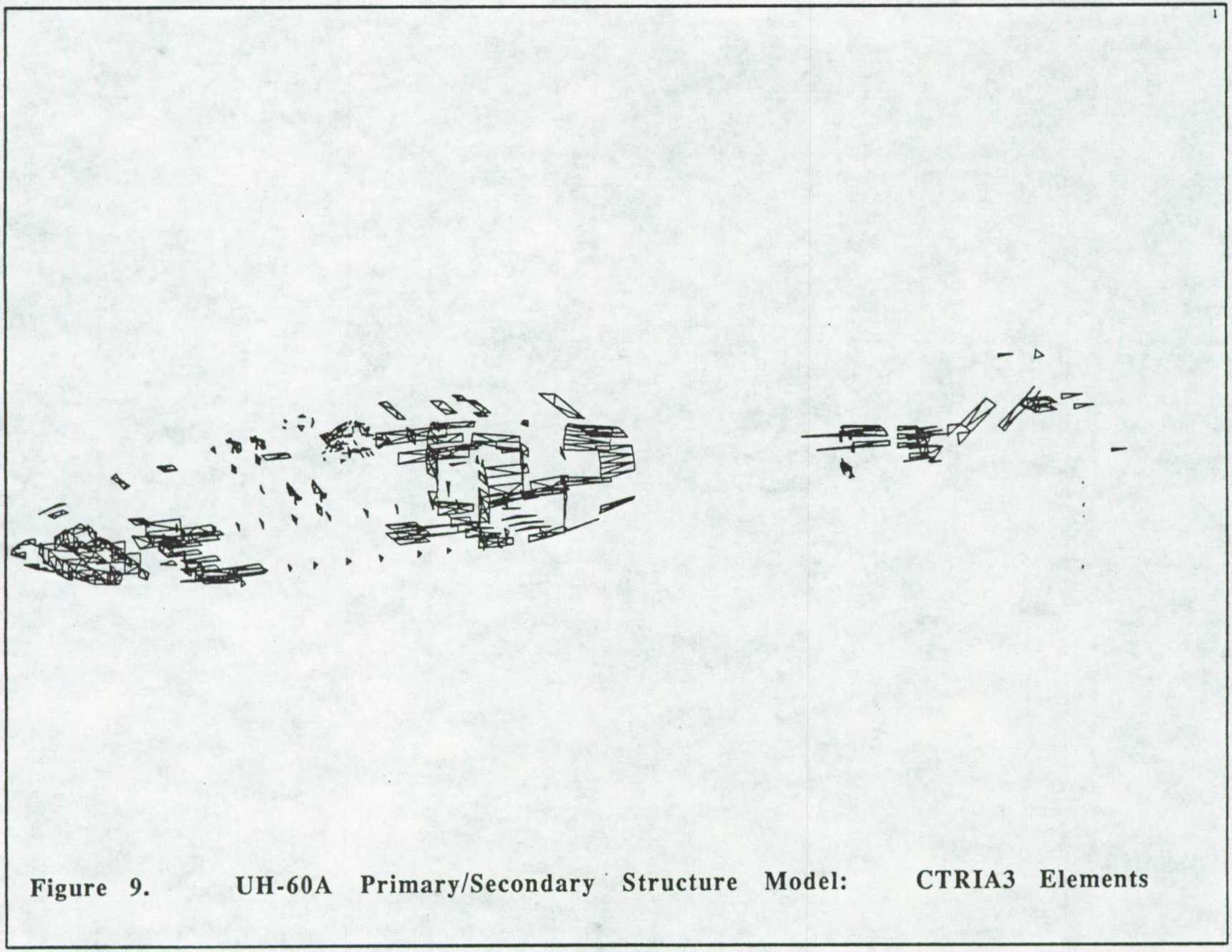

Figure 9. UH-60A Primary/Secondary Structure Model: CTRIA3 Elements

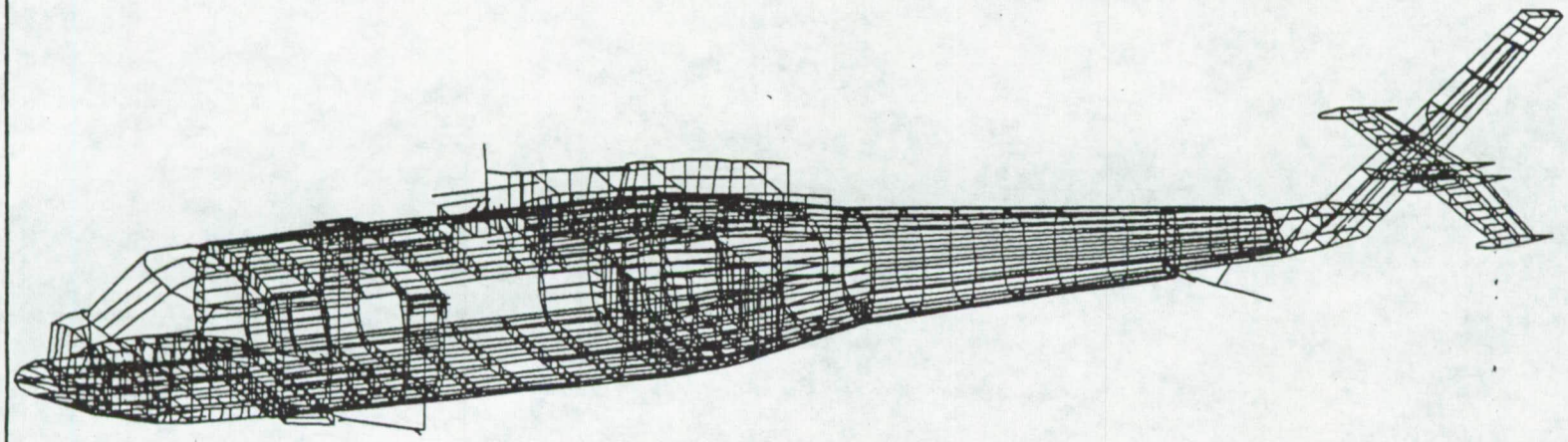

Figure 10. UH-60A Primary/Secondary Structure Model: CBAR Elements

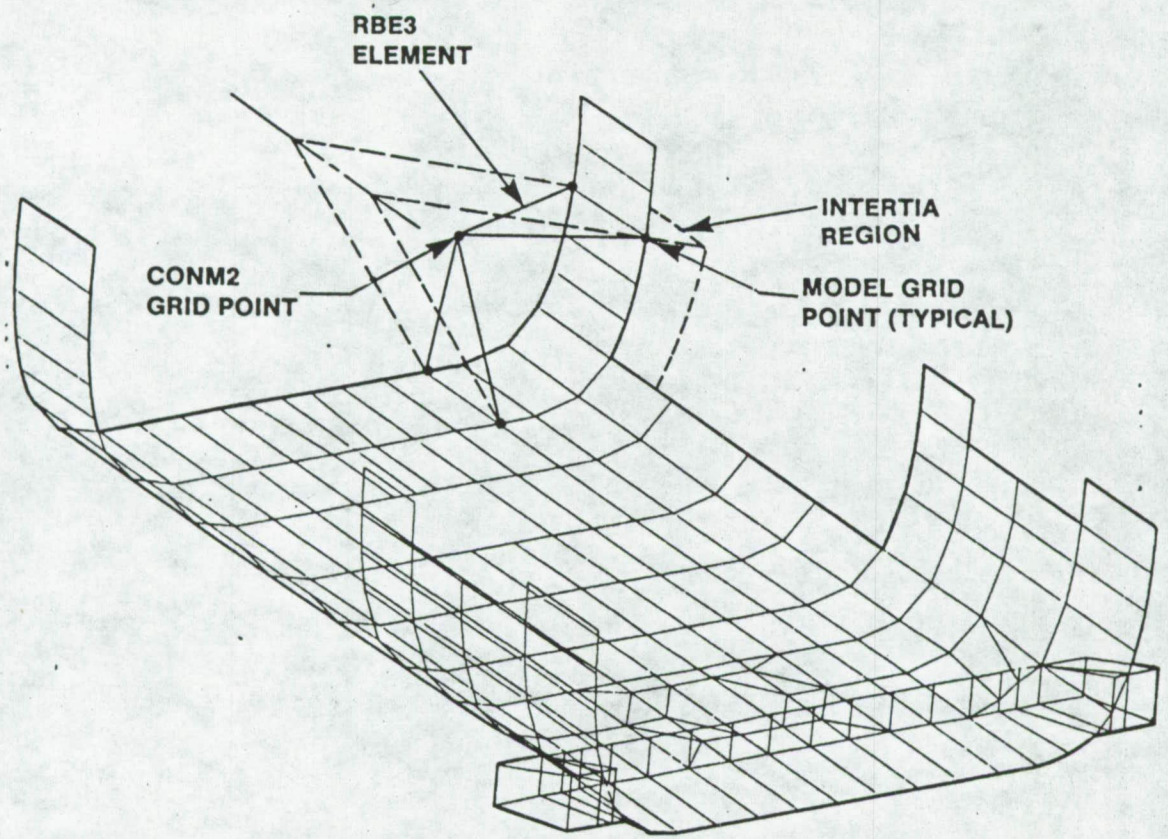

Figure 11. Mass Modeling: Representation of Distributed Mass

Prescribed Displacement $U_{longitudinal}$

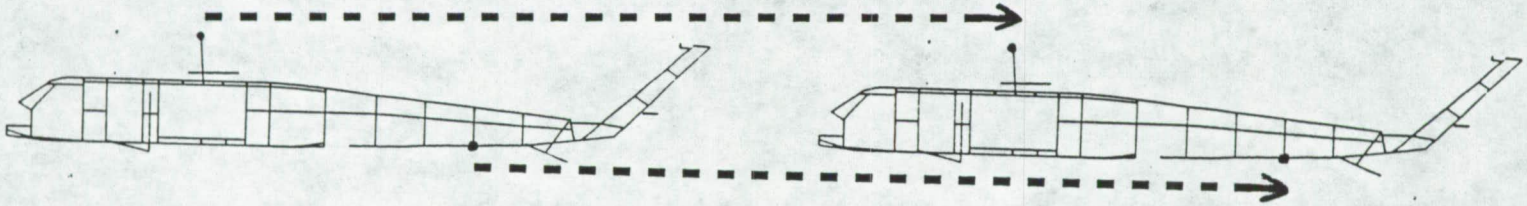

Grid Point i

Resulting Displacement $U_i = U_{longitudinal}$

Figure 12. Rigid Body Check Diagram

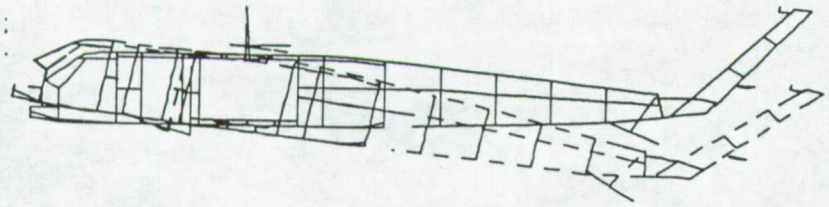

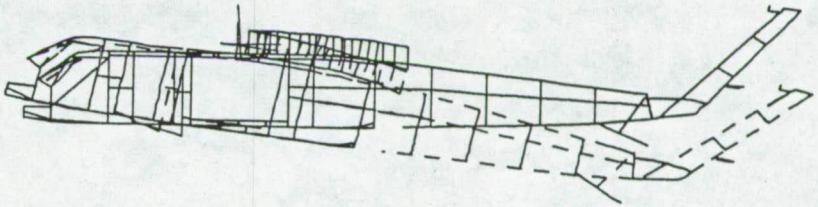

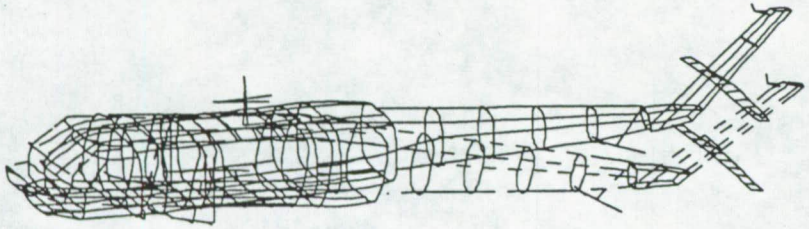

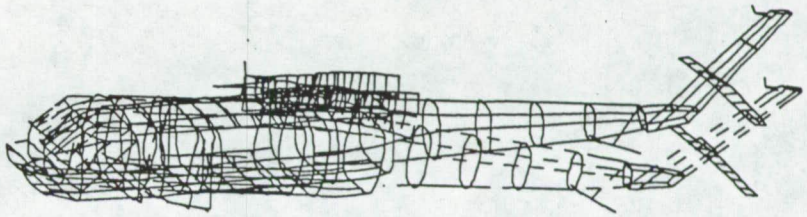

Primary Structure

Primary/Secondary Structure

Figure 13. Self Weight Load Cases

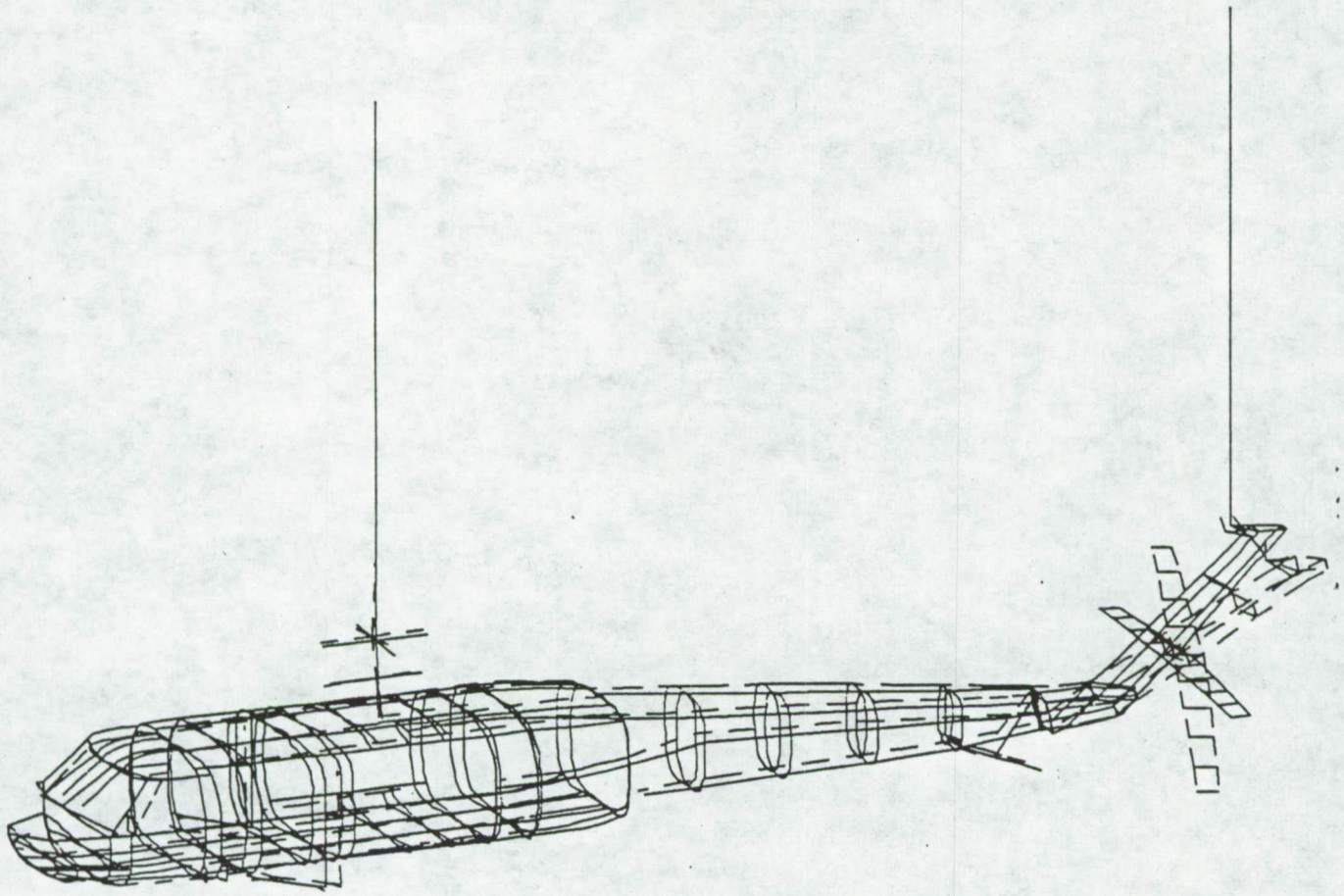

Figure 14. 1st Lateral Bending Mode (4.965894 Hz)

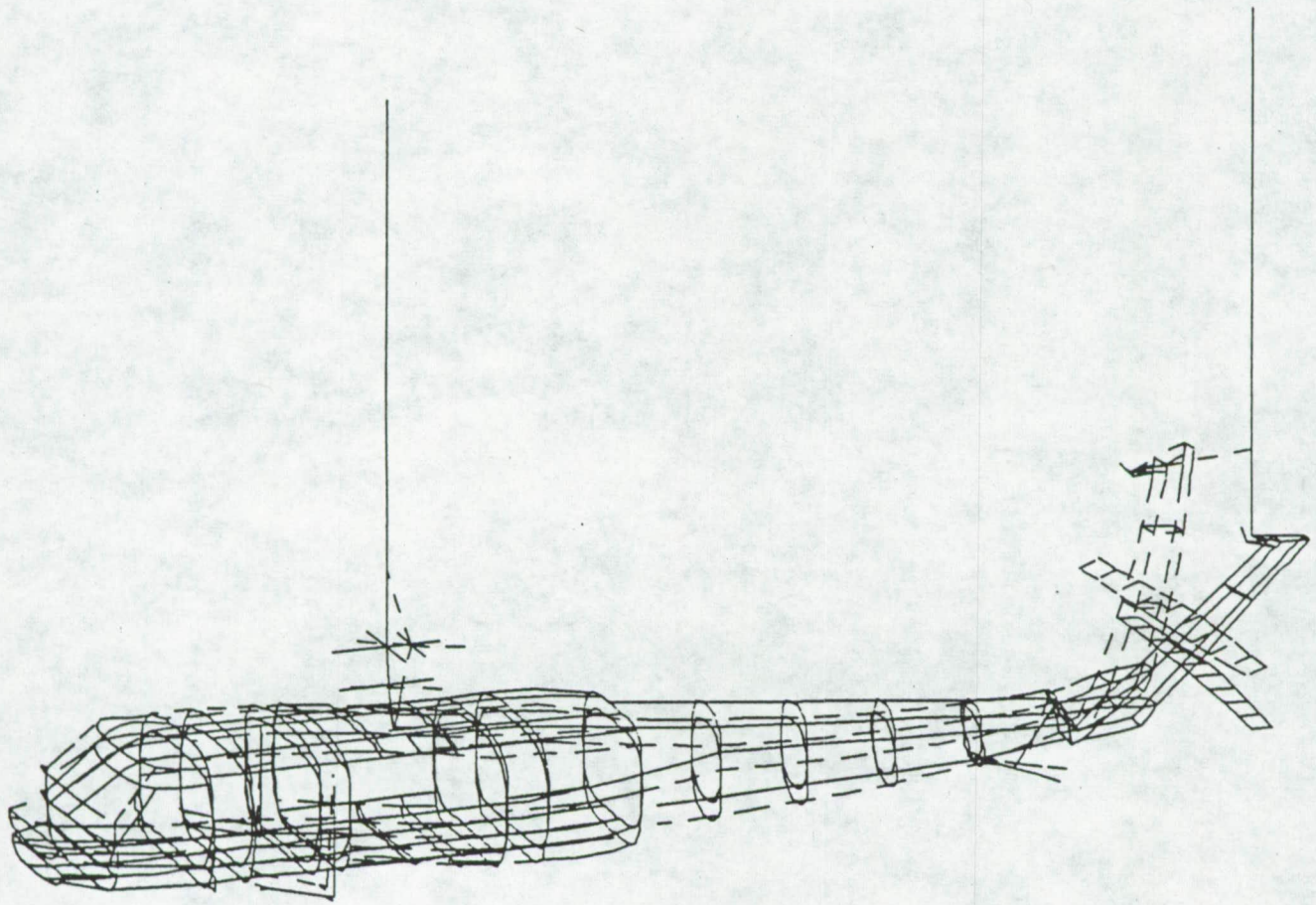

Figure 15. 1st Vertical Bending Mode (6.047724 Hz)

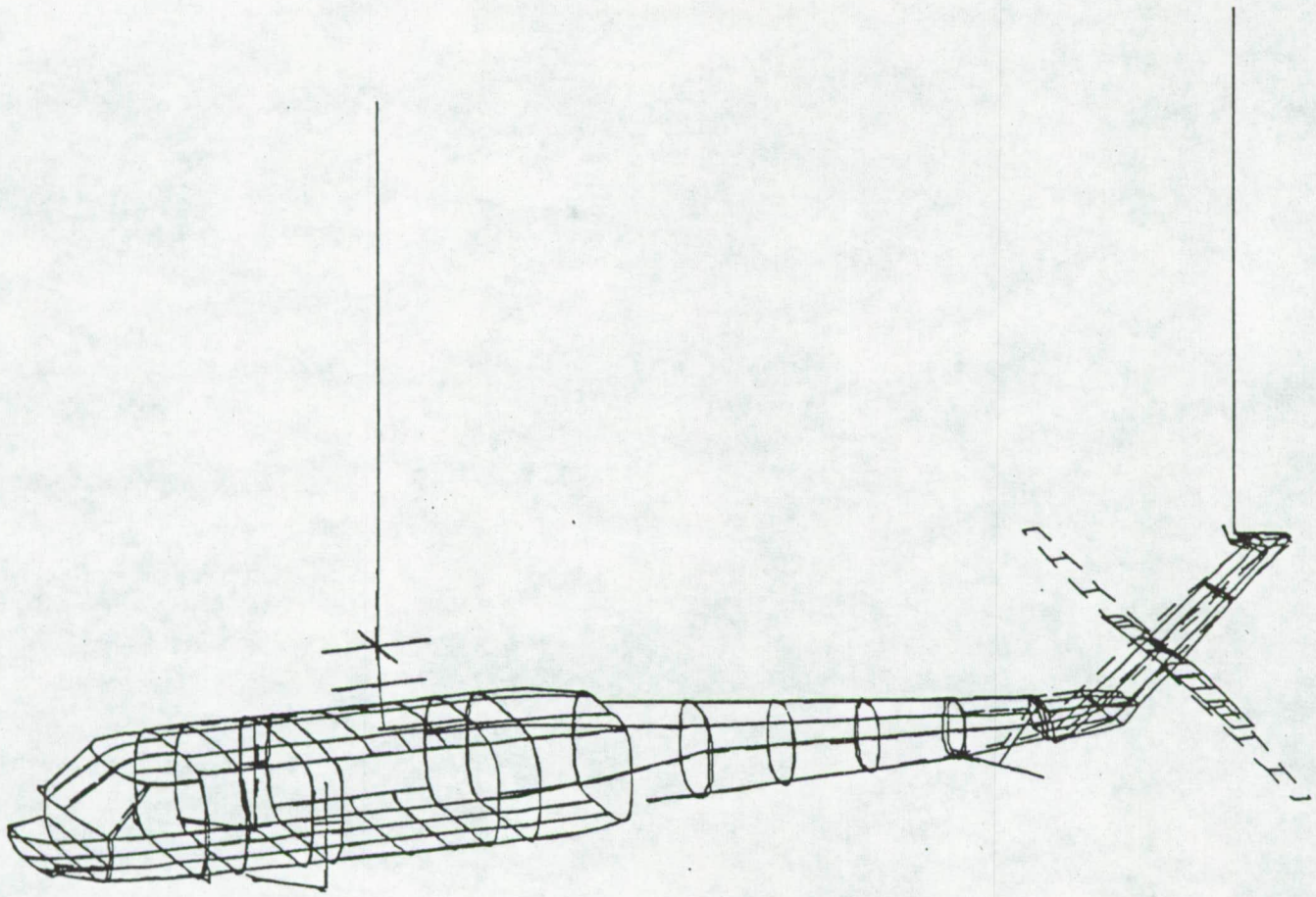

Figure 16. Stabilator Roll Mode (9.956318 Hz)

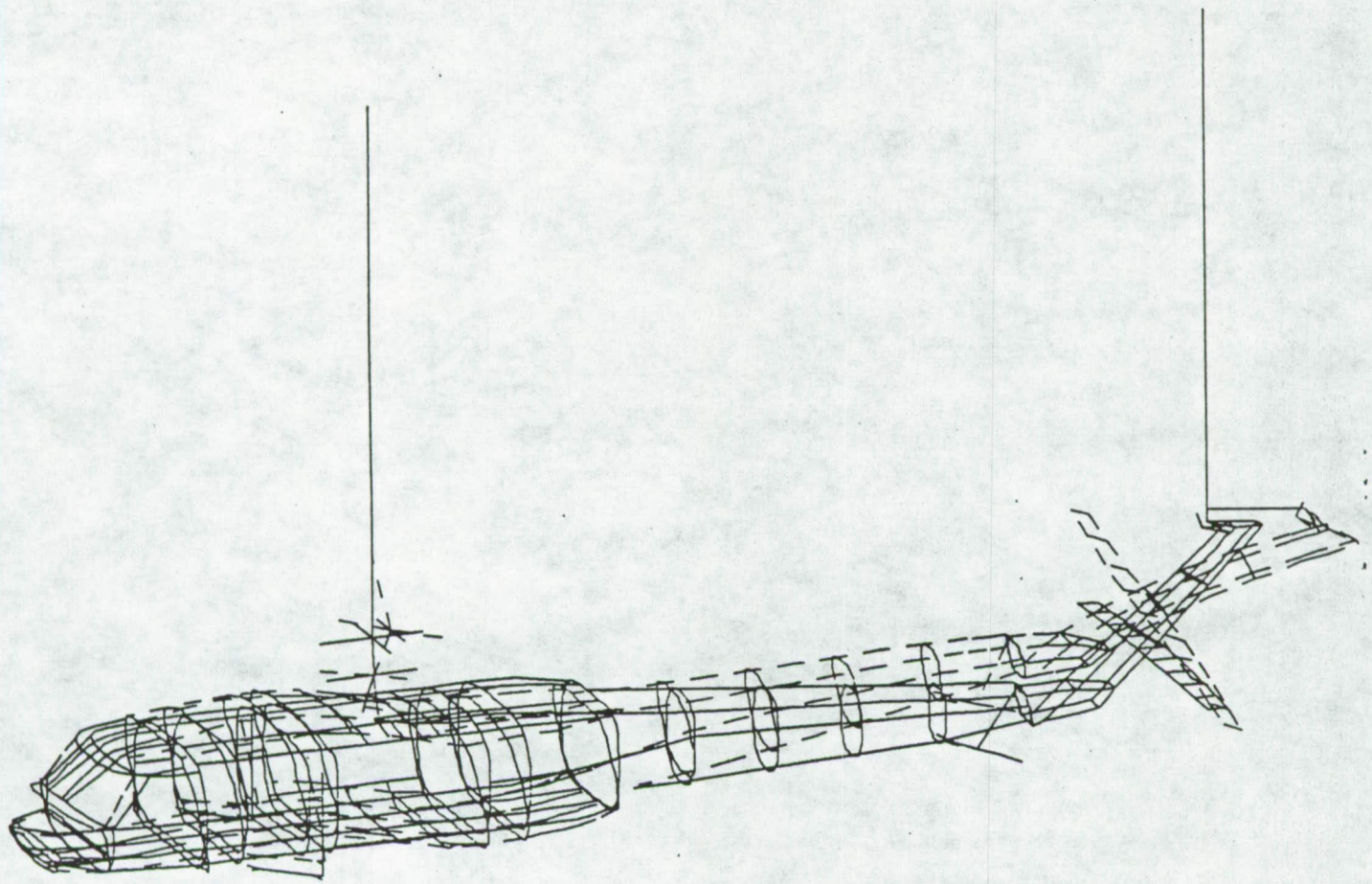

Figure 17. Transmission Pitch Mode (11.25406 Hz)

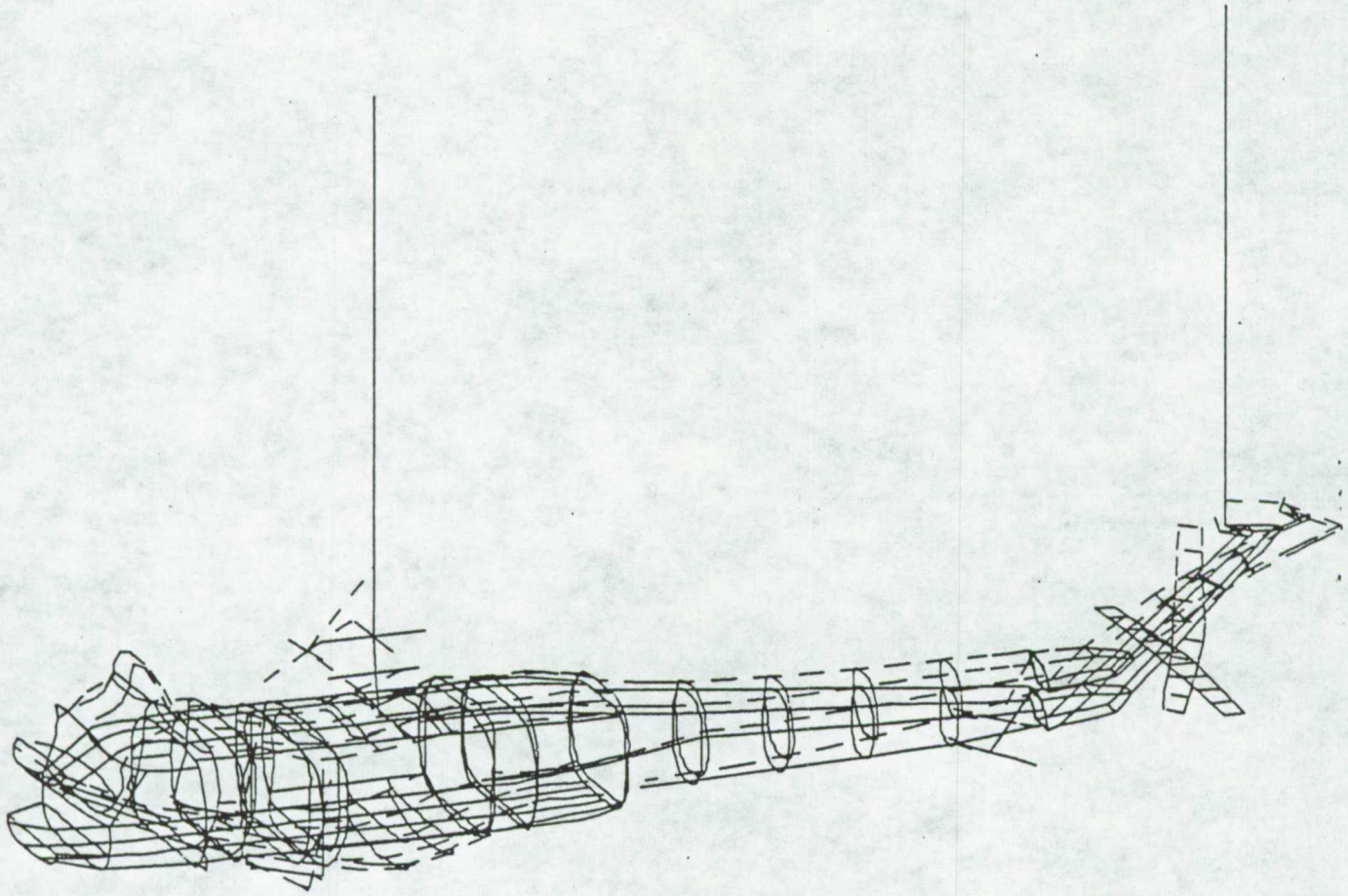

Figure 18. Transmission Pitch/2nd Vertical Bending Mode (13.07353 Hz)

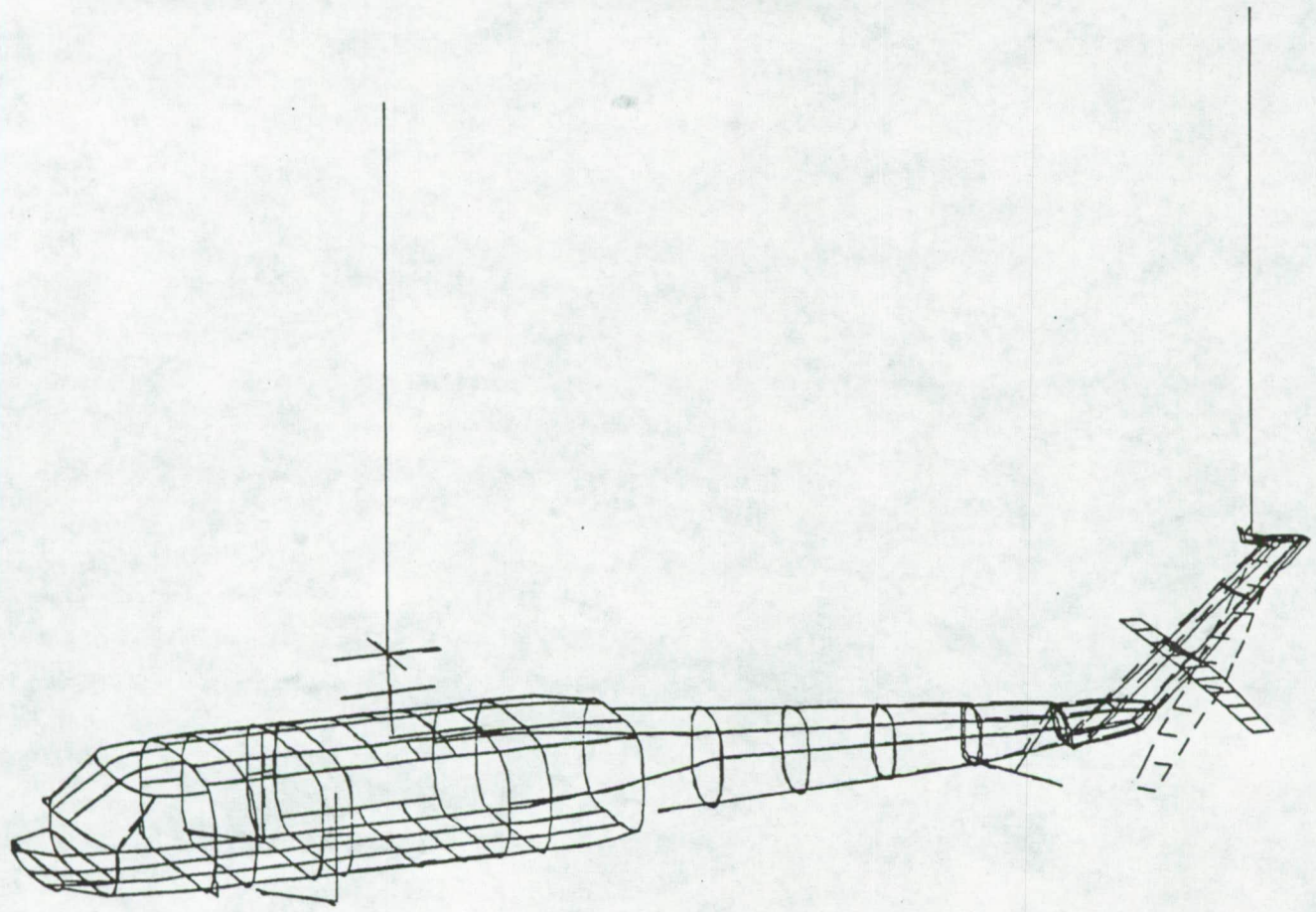

Figure 19. Transmission Roll/Stabilator Yaw Mode (13.75396 Hz)

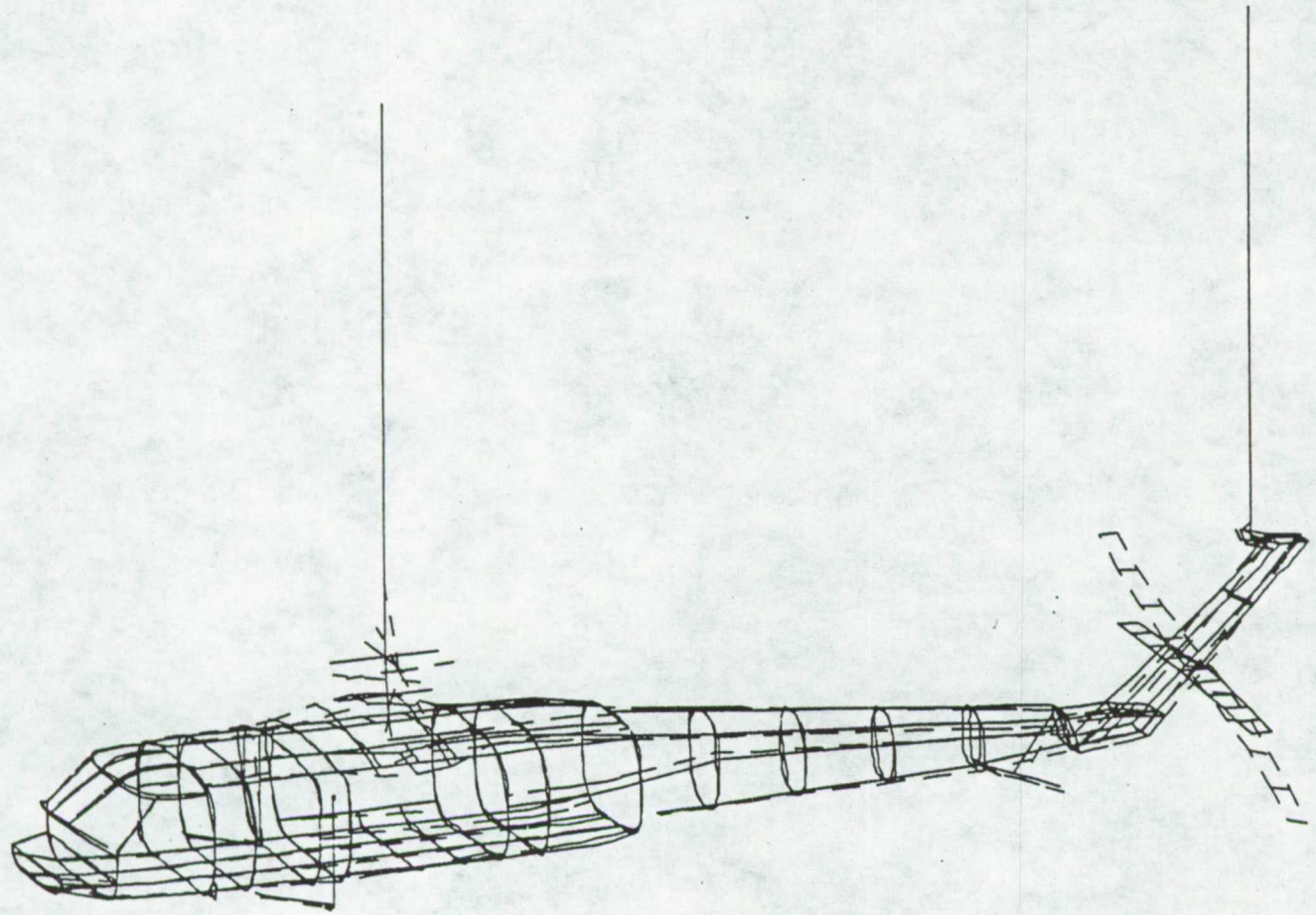

Figure 20. Stabilator Roll/Transmission Roll Mode (14.14592 Hz)

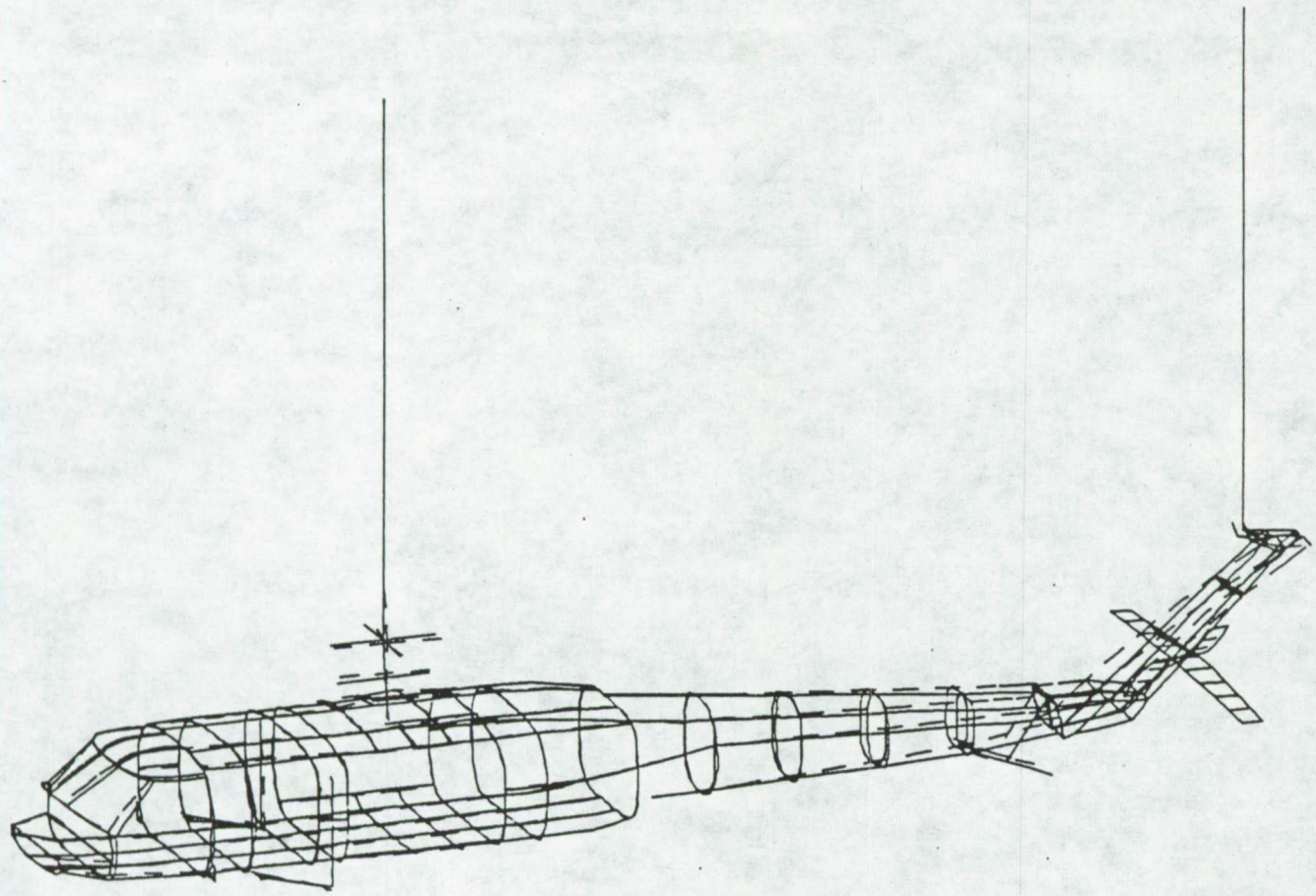

Figure 21. Transmission Roll/Stabilator Roll Mode (14.52526 Hz)

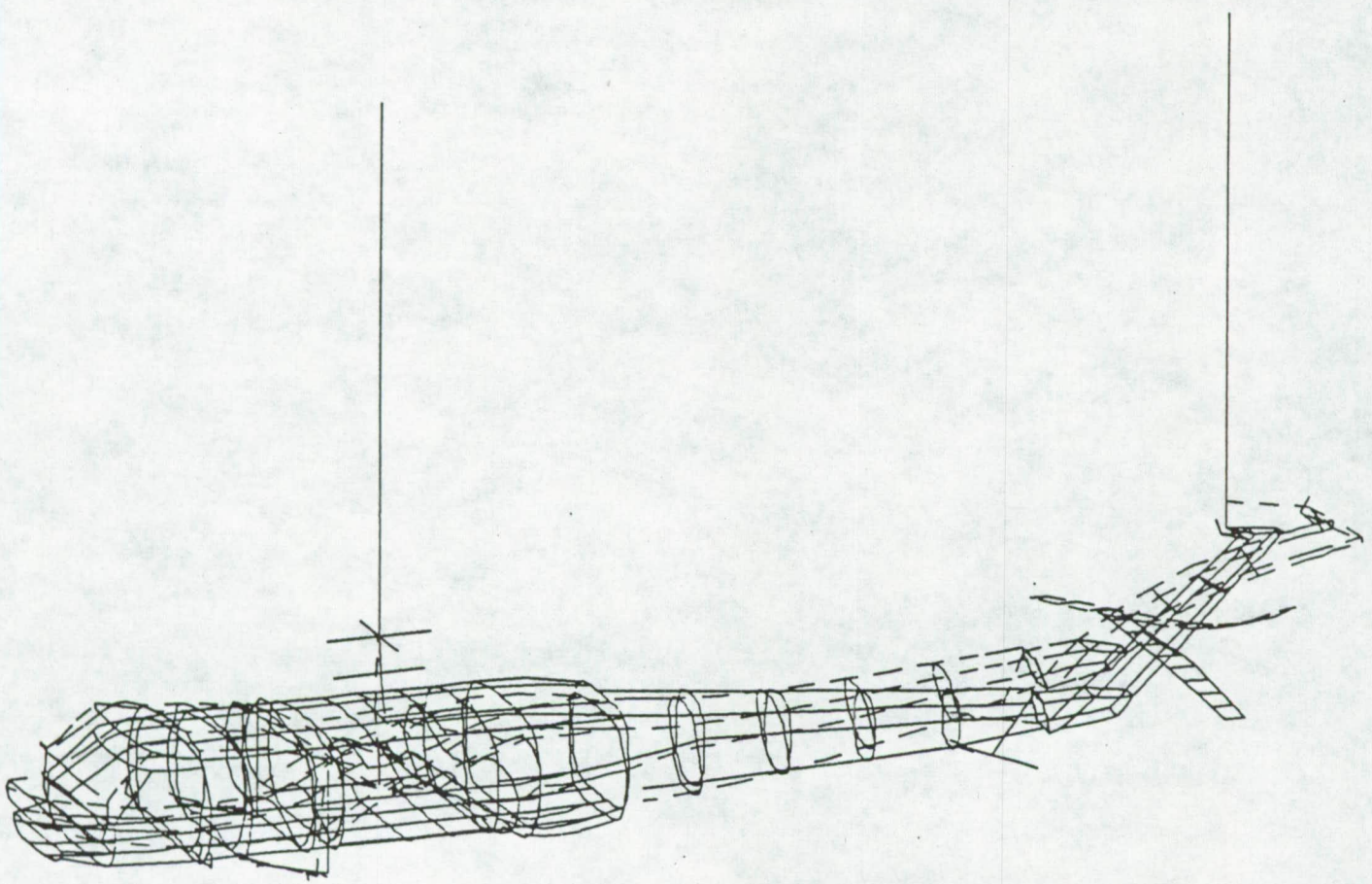

Figure 22. 2nd Vertical Bending/Transmission Vertical Mode (14.94383 Hz)

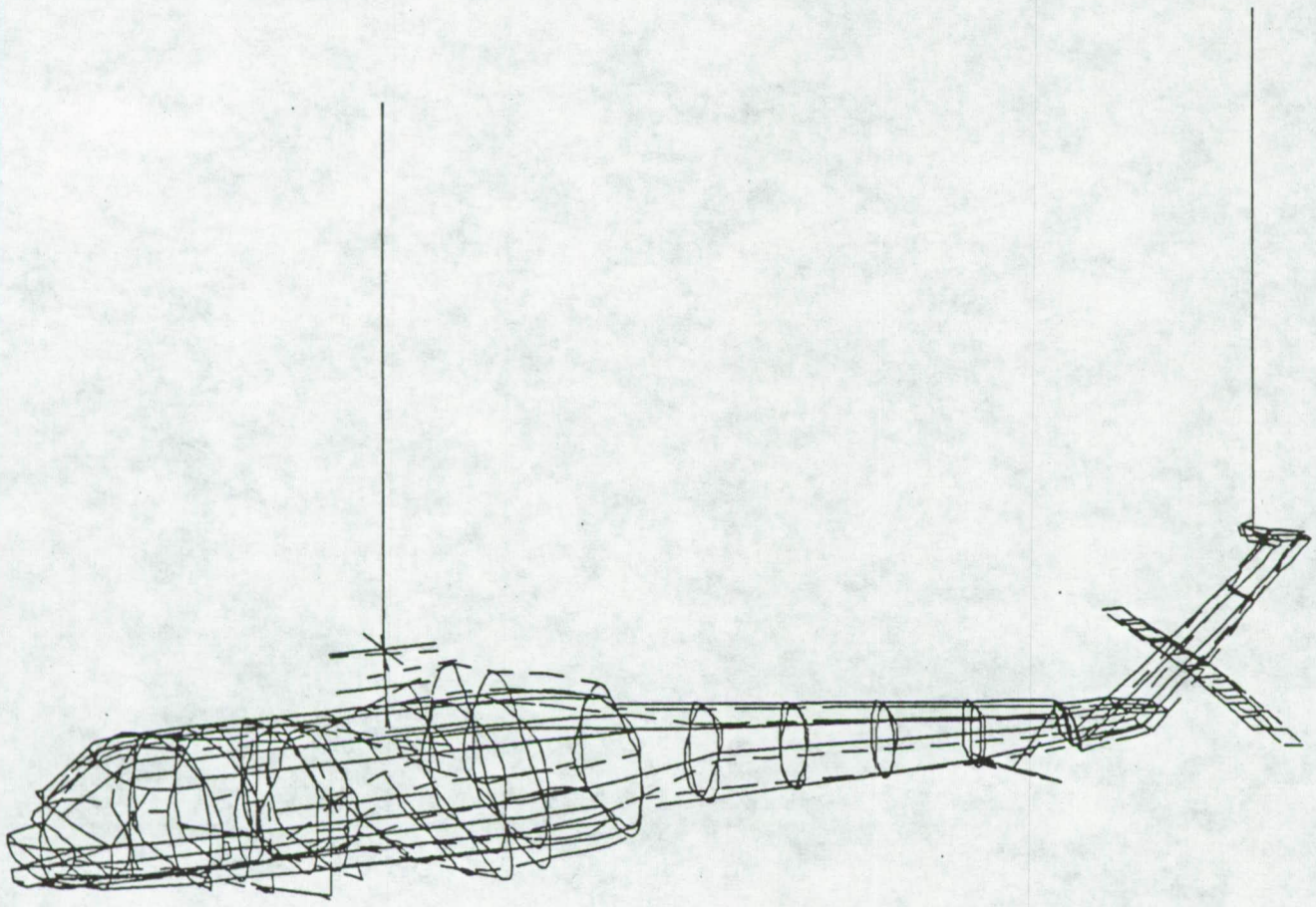

Figure 23. Cockpit/Cabin Roll Mode (17.34857 Hz)

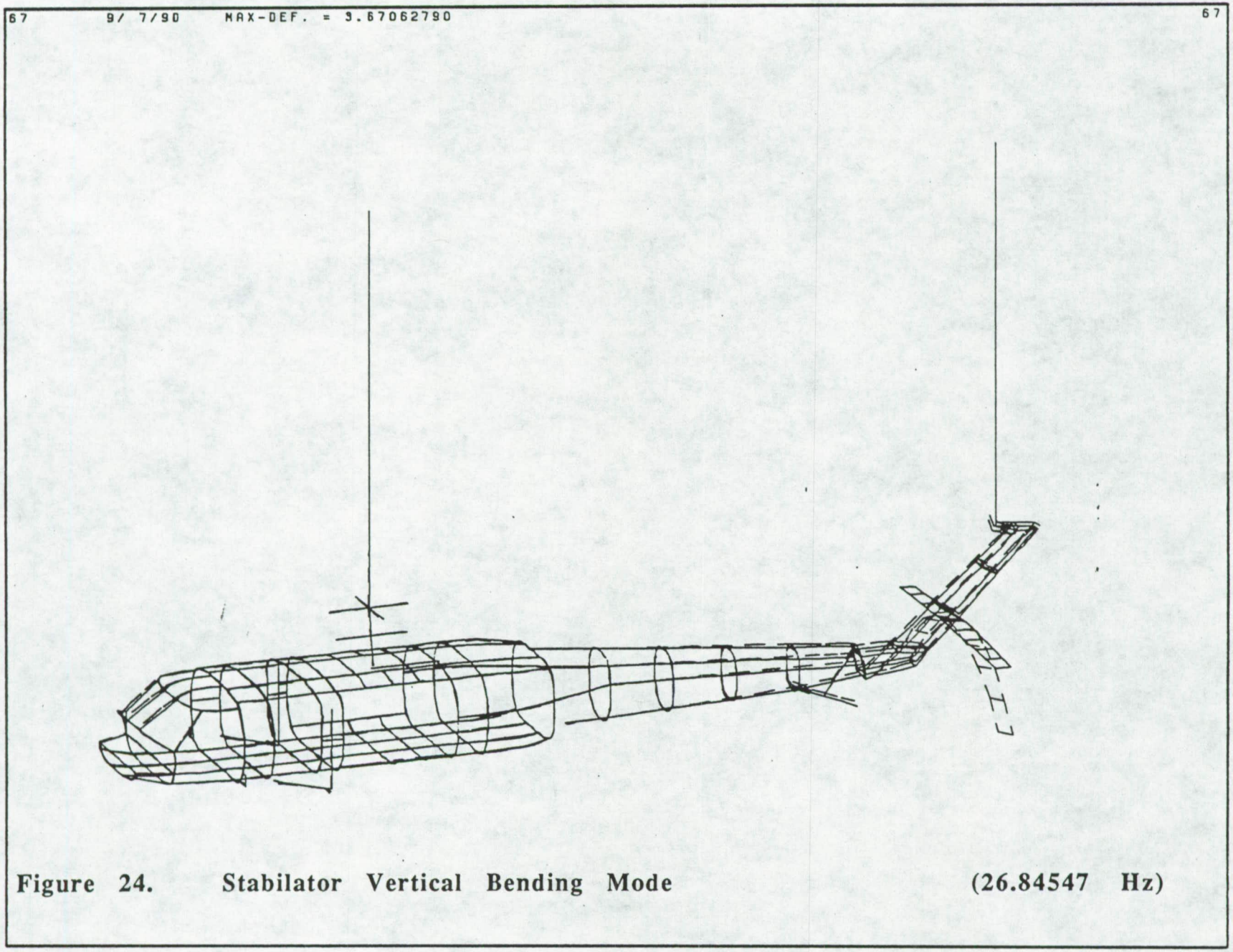

Figure 24. Stabilator Vertical Bending Mode (26.84547 Hz)

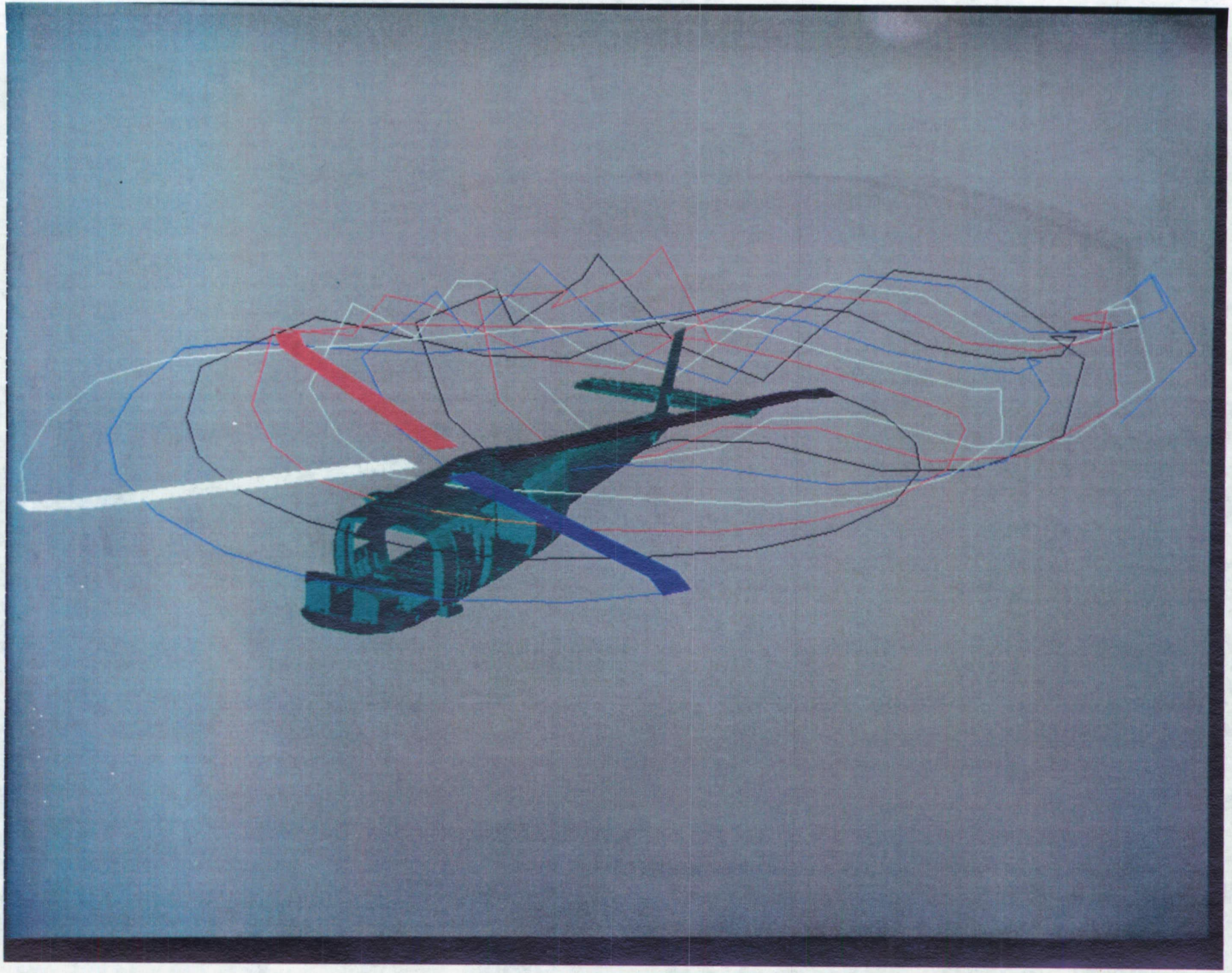

Figure 25. Visualization of the UH-60A Aerodynamic Flow Fields

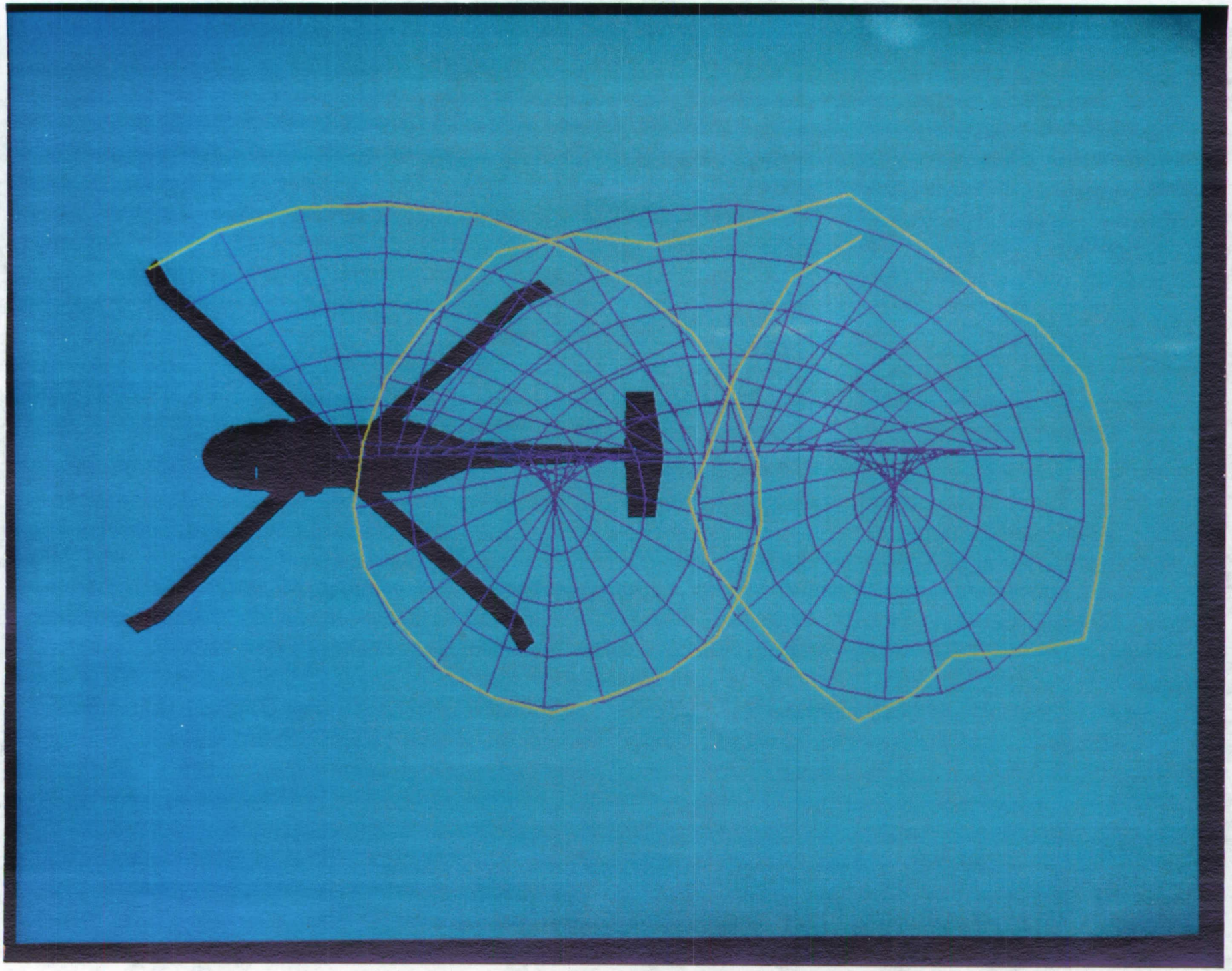

Figure 26. Visualization of the UH-60A Aerodynamic Flow Fields

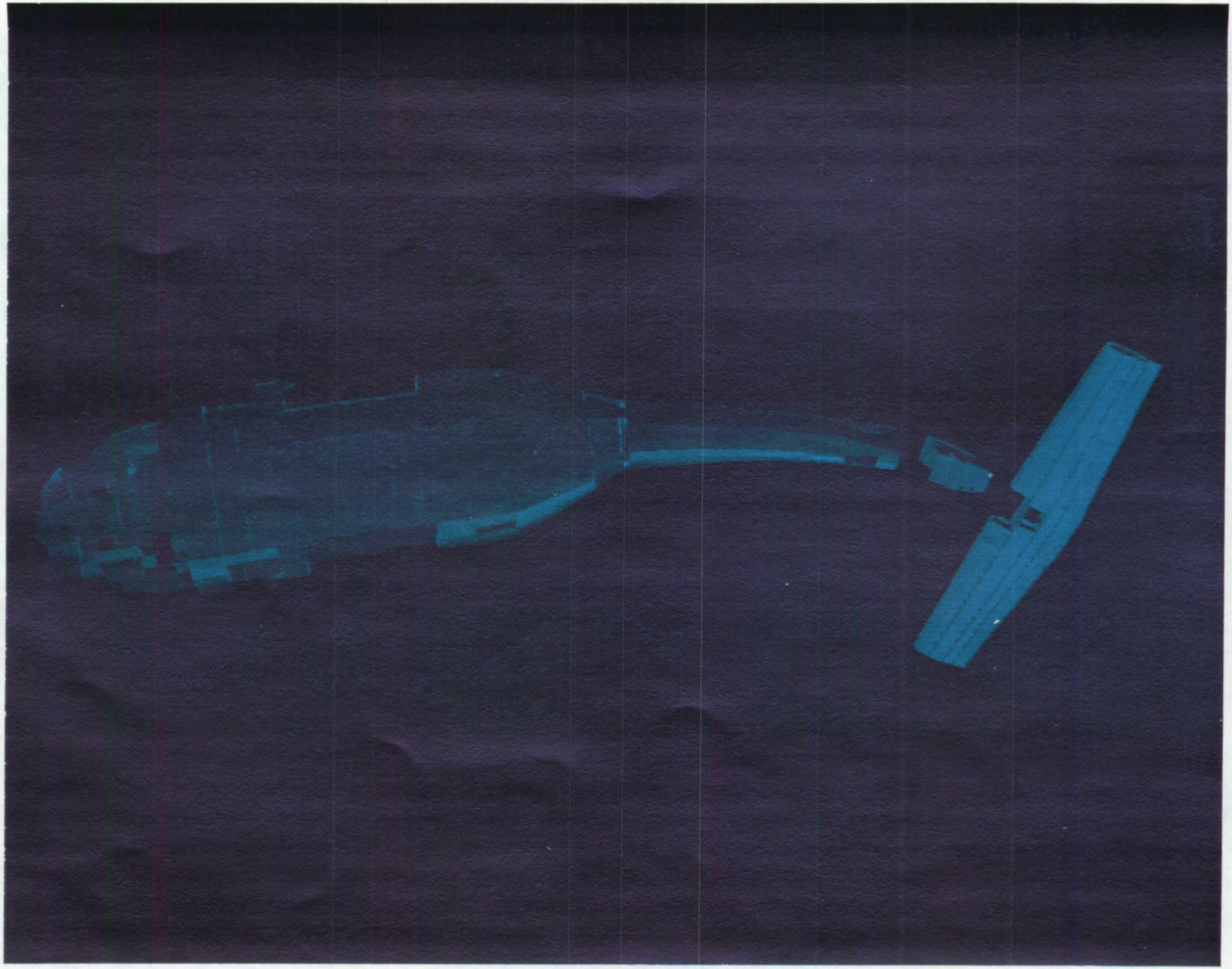

Figure 27. Animation Sequence depicting 1st Lateral Bending Mode

ORIGINAL PAGE
COLOR PHOTOGRAPH

Figure 28. Current UH-60A Rotor Airloads Flight Test Configuration

C.2

References

BRUHN, E.F. : Analysis and Design of Flight Vehicle Structures, Jacobs Publishing, Inc., Carmel, Indiana, 1973.

DIETER, GEORGE E. : Mechanical Metallurgy, McGraw-Hill Book Company, New York, New York, 1986.

DURNO, J. : Comparison of Finite Element Analysis with Shake Test Results of Sikorsky UH-60A Black Hawk, Task 3, NASA CONTRACT NASI-17499, Sikorsky Aircraft, May 1988.

DURNO, J. and MIAO, W. : Ground Vibration Test Results for NASA/AEFA Black Hawk Flight Test Configuration, Sikorsky Aircraft, Attachment to TEM-G2-7489, Enclosure (3) to Sikorsky Letter Report RSRA-PML-87-1425, Sikorsky Aircraft, September 31, 1987.

EWINS, D.J. : Modal Testing : Theory and Practice, John Wiley & Sons Inc.,New York, New York, 1984.

GABEL, R.; LANG, P.F.; SMITH, L.A.; and REED, D.A. : Plan, formulate, discuss, and correlate a NASTRAN finite element vibrations model of the Boeing model 360 helicopter airframe, NASA CONTRACT NAS1-17497, Boeing Vertol Co., April 1989.

GALLIAN, D.A. and WILSON, H.E. : The Integration of NASTRAN into Helicopter Airframe Design/Analysis, Bell Helicopter Company, 29th Annual National Forum of the American Helicopter Society, May 1973.

GOODMAN, R. and MIAO, W. : UH-60A NASA/AEFA Configuration Ground Vibration Test Results, Document SER-701619 prepared under NASA contract NAS2-13065 GW0 05, Sikorsky Aircraft, May 24, 1990.

HOWLAND, G.R., DURNO, J.A., and TWOMEY, W.J. : Ground Shake Test of the UH-60A Helicopter Airframe and Comparison with NASTRAN Finite Element Model Predictions, NASA Contractor Report 181993, NASA CONTRACT NAS1-17499, Sikorsky Aircraft, March 1990.

]HOWLAND, G.R., DURNO, J.A., and TWOMEY, W.J. : Plan, execute, and discuss vibration measurements and correlations to evaluate a NASTRAN finite element analysis model of the UH-60A helicopter airframe, Task 3 Report, NASA CONTRACT NAS1-17499, Sikorsky Aircraft, October 1986.

HOWLAND, G.R., DURNO, J.A., and TWOMEY, W.J. : Plan, formulate, and discuss a NASTRAN finite element model of the UH-60A helicopter airframe, Task 2 Planning Report, NASA CONTRACT NAS1-17499, Sikorsky Aircraft, September 1984.

KILROY, K.L. : Planning, Creating, and Documenting a NASTRAN FEM, Results and Experiences, Task 2, NASA CONTRACT NAS1-17498, Hughes Helicopters, Inc., September, 1985.

KVATERNIK, R.G. : Langley Rotorcraft Structural Dynamics Program - Background, Status, Accomplishments, Plans, NASA TM 101618, June 1989.

MACNEAL-SCHWENDLER CORPORATION - Edited by M.A. Gockel : MSC/NASTRAN Handbook for Dynamic Analysis, Version 63, June 1983, c.1983.

MACNEAL-SCHWENDLER CORPORATION - Edited by R.H. MacNeal : MSC/NASTRAN Handbook for Linear Analysis, Version 64, August 1985, c.1985.

MACNEAL-SCHWENDLER CORPORATION : MSC/NASTRAN User's Manual, Vol. I & II, Version 65, November 1985, c.1985

RICH, MELVIN J. : Finite Element Analysis of Helicopter Structures, Sikorsky Aircraft

SCHAEFFER, HARRY G. : MSC/NASTRAN Primer, Wallace Press, Inc., Milford, New Hampshire, 1979.

TWOMEY, W.J., CHEN, T.L.C., OJALVO, I.U., AND TING, T.I. : Application to a Helicopter of a general method for modifying a finite element model to correlation with modal test data, : Proceedings of the AHS National Specialist's Meeting on Rotorcraft Dynamics, Arlington, Texas, November, 1989.

Acknowledgments

To Javier Escobedo for his respective work effort regarding this study.

To Tim Cheng of Sikorsky Aircraft for his continued efforts in making UH-60A modeling data available to the Rotorcraft Technology Branch.

To the National Science Foundation for the supplementary use of San Diego Super Computer Facilities needed for these analyses.